UNIVERSITY OF GÄVLE

FACULTY OF ENGINEERING AND SUSTAINABLE DEVELOPMENT
Department of Computer and Geospatial Sciences

Evaluation of SLAM based mobile laser scanning and terrestrial laser scanning in the Kiruna mine

A comparison between the Emesent Hovermap HF1 mobile laser scanner and the Faro Laser Scanner Focus 3D X 330 terrestrial laser scanner

Claes Gustafsson & Anton Lukkarinen

2023

Degree project, Basic level (Bachelor degree), 15 HE
Surveying Technology
Study Programme in Land Surveying

Supervisor: Ulrika Ågren
Examiner: Faramarz Nilfouroushan

Abstract

The mining industry has over the last few decades seen a drastic increase in the usage of laser scanning technologies as a way of creating 3D maps of the mines being exploited. Underground mapping in places such as mines has become more prevalent as the technology has progressed and made it easier to generate highly detailed point clouds faster. A newer and faster method of generating point clouds is using a simultaneous localization and mapping (SLAM) based mobile laser scanner (MLS). With the help of complex algorithms, it enables instant point cloud registration and allows for continuous mapping of the surrounding environment while tracking the device location without needing a connection to GPS. As the accuracy and speed of SLAM based MLS continues to improve, its use is becoming far more widespread within the mining industry. Although studies have been conducted previously investigating the differences in quality between SLAM based MLS and terrestrial laser scanners (TLS), there is still a need for further studies conducted in mining environments. This case study aims to investigate the quality differences between two point clouds generated using an Emesent Hovermap HF1, which is a SLAM based MLS, and a Faro Laser Scanner Focus 3D X 330 TLS. Parameters like root mean square (RMS) were investigated. Volume calculations were carried out for both point clouds and compared to each other as well the calculated volume of a theoretical model. To conduct this study data from LKAB's Kiruna mine was collected and provided by Blå Projekt, Process & GIS AB.

The result of this study concludes that the Faro TLS is superior in terms of point cloud quality, with five times better RMS values and higher point density than the Hovermap MLS. It also shows that both scanners allowed for accurate volume calculations with only roughly 1% difference in the estimated volumes. The TLS method yielded a much more readable point cloud with clearer visual details than the SLAM based MLS method. This may however be a result of SLAM drift since no loop closure was performed when collecting the MLS data which otherwise could've minimized the errors.
It was concluded that due to the amount of data processing required and the longer work time of TLS, SLAM based MLS is a method that is worth further development as it provides unparalleled flexibility, safety improvements and work time efficiency.

Keywords: *Terrestrial laser scanning, mobile laser scanning, simultaneous localization and mapping, underground mapping, Kiruna mine.*

Preface

Firstly, we would like to offer our sincerest gratitude to Bo and Henrik Fjellborg at BLÅ Projekt, Process & GIS AB for providing us with the data which we used for our case study and for their continued support throughout the project. Without your support this bachelor's thesis would not have been possible.

Secondly, we would like to thank Ulrika Ågren, our project supervisor who was instrumental in helping us with putting together and structuring this paper as well as possible.

We also want to extend our gratitude towards Faro, that kindly provided us with free trial versions of their SCENE software.

Lastly, we want to say thanks to Högskolan i Gävle and our wonderful teachers and professors that we've had the pleasure of meeting during these last few years. It has been a wonderful and highly educational time for us.

Table of contents

Abstract i
Preface iii
Table of contents v
1 Introduction 1
1.1 Background 1
1.2 Purpose and research questions 2
1.3 Project limitations 3
1.4 Ethical aspects 4
2 Theory 5
2.1 Registration and georefencing 5
2.2 Use of 3D laser scanners in the mining industry 6
2.2.1 SLAM based scanners in the mining industry 7
2.3 Different kinds of SLAM 8
2.3.1 SLAM with LIDAR incorporated WILDCAT 9
2.4 HMK regulations 9
3 Methodology 11
3.1 Software and materials: 11
3.2 Instruments 12
3.3 Study Area 13
3.4 Data collection by Blå Projekt, Process & GIS AB 14
3.5 Initial data processing 16
3.5.1 Faro Laser Scanner Focus 3D X 330 data processing 16
3.5.2 Emesent Hovermap data processing 17
3.6 Georeferencing the point clouds 17
3.7 Visual inspection 18
3.8 Volume calculation 19
4 Results 20
4.1 Registration of Faro scans 20
4.2 Geoprocessing point clouds 21
4.3 Point cloud quality visual inspection 25
4.4 Calculated volumes 29
5 Discussion 34
5.1 Comparison of point clouds 34
5.2 Interpretation of results 35
6 Conclusions 38
7 Future studies 40
References 41
Appendix A A1
Appendix B B1
Appendix C C1

Appendix D D1
Appendix E E1
Appendix F F1

1 Introduction

1.1 Background

Terrestrial laser scanning was developed during the 1970s and is based around LIDAR technology. LIDAR is a technology in which laser pulses are emitted onto a surface and the time it takes for these pulses to return is measured, this way it is possible to measure the distance between the device and the surface (Kekec et al., 2021).

In the 1990s this technology started being implemented in geodetic instruments as a reflectorless distance measurement method (Reshetyuk, 2006). The use of TLS technologies in the mining industry has increased drastically over the last decade as the advances in these technologies allow for accurate, fast, and high-resolution data collecting. The resulting point clouds are highly detailed and are used by mining corporations to create models and meshes of tunnels and chambers in the mine. Tunnel models are compared to theoretical models for size comparisons to make sure that the tunnels are neither too big nor too small which can become very expensive to correct. Meshes are used as a basis when miners plan where to drill holes in the mine to place explosives. Point clouds are also turned into 3D models which are used to display information about the mine environment, improving productivity and safety. When working with stationary laser scanners the operator sets up the instrument and collects data from the surrounding terrain, the instrument is then moved to a different location and collects data from the new position. This way an overlap is formed between the scans which enables for a more accurate registration of the resulting point clouds. This can be a timely process however, since the operator needs to horizontalize the instrument each time it is moved to a new location, and it is also important to keep an adequate distance between each station set up in order to maintain a good overlap. There also needs to exist visible targets in each of the captured scans in order to assure a good registration between each captured scan, these targets are often in the shape of spheres placed on tripods or rectangular plates with a checkerboard pattern.

These processes all require some pre-planning before the data collecting can begin and so even if stationary TLS methods have been proven to be highly accurate the process of collecting and processing data can be very time consuming. SLAM (Simultaneous Localization And Mapping) is a method which opened up several possibilities for mapping caves with TLS and as the technology becomes more affordable, more companies are investing in SLAM equipped MLS (Mobile Laser Scanner) devices. The major benefit with SLAM technology is that the device can map an area while simultaneously identifying its own position by using SLAM algorithms. This eliminates the need to have several set ups for the scanner and

allows for a faster mobile mapping experience. According to Gollob et al. (2020), a surveying task performed with a SLAM equipped scanner can at present date be almost five times as fast compared to working with a stationary scanner. SLAM devices can be handheld, fit on backpacks and on vehicles, both remote and manually driven. This is important in cave mapping as areas which are deemed unstable or otherwise not safe for personnel to be in can be mapped via remote controlled vehicles, such as robots or drones, equipped with a SLAM laser scanner. Comparing the results of a modern SLAM based MLS device with a traditional stationary TLS in the mining industry is important as stationary laser scanners are widely regarded as more accurate and able to capture more detailed scans than mobile scanners. As SLAM technology has continued to improve this gap in quality between the two methods has decreased. SLAM based scanners are now able to produce point clouds of sufficient quality to be used by the mining industry and offer a safer, more flexible, and user-friendly working method.

1.2 Purpose and research questions

The goal of this bachelor's thesis is to compare 3D point clouds of a mining tunnel created by a stationary Faro TLS and a SLAMbased Emesent Hovermap handheld MLS. The point clouds will be compared to determine what the differences in terms of quality there are between the two types of laser scanners. The mining tunnel is located in a mine in Kiruna and the collected data has been supplied by BLÅ Projekt, Process & GIS AB. The part of the tunnel where the data was collected is a curved section of a larger tunnel system. The mining tunnel is sparse in details and has a very monotone interior appearance, this means that there are few distinct common points for the laser scanners to use as help with scan registration, except for reference points and targets. The shape of the tunnel will thus test both scanners' abilities to capture, register and produce detailed point clouds in a challenging mining environment. The Faro Focus3D X 330 laser scanner has a measurement rate of up to 976 000 points per second (FARO, 2015) while the Emesent Hovermap has a measurement rate of 300 000 points per second (Emesent, 2022). This means that in theory the Faro scanner should produce more detailed point clouds than the Hovermap scanner, however the Hovermap generated point cloud may prove detailed enough and thus unwarant the longer and more tedious working time with the Faro scanner. This would mean that the Hovermap scanner is a better option for mapping cave tunnels as SLAM is a very time effective method for capturing scanning data and the incorporated WILDCAT SLAM technology of the Hovermap has been designed to aid the device in challenging environments (Emesent, 2022). Another possibility is that the details of the Hovermap generated point clouds won't be high enough to allow for easy reference point recognition in the cave tunnels and this would mean that the stationary Faro scanner is better

suited for mining operations. The quality of the point clouds will be assessed by the quality of georeferencing, the calculated volumes and the visual quality. The quality of georeferencing will be judged based on the given RMS (Root Mean Square) value given when a point cloud is georeferenced. Each point cloud will have its volume estimated by manual calculation and by software. These estimated volumes will then be compared to each other and to the values of the other point cloud to see if there are any differences. Lastly the visual quality of each point cloud will be judged based on the ability to identify certain objects within the point clouds. By comparing these factors this bachelor's thesis aims to investigate which scanner is best suited for mining industry related tasks.
This bachelor's thesis aims to answer the following questions:

- Which of the two laser scanners Faro Focus3D X 330 TLS and Emesent Hovermap HF1 MLS produces the highest quality point cloud of a curved mining tunnel, with regards to RMS values, number of points, point density, visual clearance, and the ability to display visual details?

- Does the calculated volume of a point cloud of a curved mining tunnel created with a Faro Focus3D X 330 TLS, and one created with an Emesent Hovermap HF1 MLS differ from each other and a volume calculated from a theoretical planned model?

1.3 Project limitations

This bachelor's thesis will focus on comparing two specific laser scanners: the Faro Focus3D X 330 TLS and the Emesent Hovermap. Many other laser scanners exist which could have been compared but these two models are the ones used by the company which provided the data used in this bachelor's thesis and therefore these two models will be compared to each other. The Faro Focus3D X 330 TLS was released in 2010 while the Emesent Hovermap was released in 2021. This means that the Hovermap is a much more modern state of the art laser scanner compared to the Faro. This bachelor's thesis will not consider the age difference between these two models as a SLAM based MLS from 2010 would not be powerful enough to generate a detailed enough point cloud in such a challenging environment as a curved mining tunnel. The two scanners used are both being used in today's mining industry and therefore it is applicable to compare the models. The quality of georeferenced point clouds is usually tested by picking checkpoints in the point cloud and comparing the change in coordinates of the checkpoints in the georeferenced point cloud with the known values. As the data that was delivered for this bachelor's thesis did not contain information about checkpoints, this step in the quality control is not able to be performed. There is no known true value of the scanned tunnel section used in this project and therefore it is not possible to

compare the calculated volumes to a known value, instead these values will be compared to each other, and a theoretical tunnel based on what the mining company LKAB intended to create to see if the two laser scanners produce different calculated volumes.

This bachelor's thesis will be limited to comparing only the quality of a single section of a larger mining tunnel as the environment is almost identical in all parts of the larger tunnel, the results produced by the chosen scanners can easily be replicated in similar mining operations and the results would be applicable there as well. Furthermore, as the point clouds contain large amounts of data that require very large processing power, the point clouds will require subsampling for some of the comparisons as the hardware requirements for processing the entire point clouds are not available. This should however have little to no impact on the result.

1.4 Ethical aspects

Since this bachelor's thesis will be comparing two different laser scanners produced by two different companies it is important to remain impartial and not show bias towards any company or model. The data was collected by an impartial third company which means that it can be assumed to not show bias towards any one of the used devices. It is also important to not show bias towards the more modern and advanced SLAM based device. It can be easy to unconsciously elevate the capabilities of a new and interesting device or technology which is changing the work field in a positive way, but this bachelor's thesis must still remain objective towards the research questions.

This bachelor's thesis is a case study between the two specific laser scanners, the Faro Focus3D X 330 and the Emesent Hovermap, set in a very specific environment and only focusing on comparing specific factors in point clouds. To draw conclusions regarding these two scanners more case studies need to be carried out.

2 Theory

2.1 Registration and georefencing

Stationary laser scanners capture and produce individual scans that need to be registered together to create a single coherent point cloud that can then be georeferenced. There exist two primary methods for doing this as explained in HMK-Terrester laserskanning, (2015). The first method is the indirect georeferencing method which produces the lowest uncertainty and can be divided into the one-step technique and the two-step technique. In the one-step technique each individual point cloud is georeferenced which then creates a combined point cloud; the advantage with the one-step technique is that there is no need for any overlap between each scan.

In the two-step technique each scan has a minimum overlap of 30% in which placed signals or natural common connection points enable the scans to be registered and georeferenced. It is also possible to directly register point clouds to point clouds with the so-called point cloud registration technique. It is necessary to have at least four connection points within the overlap to allow for high quality registration and that these points are placed in three orthogonal angles. When georeferencing it is necessary to use at least five different reference points that are spread out and not in the orthogonal line (HMK-Terrester laserskanning, 2021).

The second method is called the direct georeferencing method where the laser scanner must be equipped with a compensator. Two different techniques can be used for this method: the traverse technique or the known backsight technique. In the direct georeferencing method there is no need for any overlap and the scanner's position and orientation are directly entered in a geodetic reference system. With the known backsight technique, the scanner and backsight are both centered and levelled over connection points on the ground and instrument- and signal heights are measured. The traverse technique works much the same as when measuring with a total station in that forced centering has to be used and each scan position around the object is planned in such a way that a closed chain is formed (HMK-Terrester laserskanning, 2015).

With the SLAM based MLS there is no need for any manual registration, the MLS instead automatically registers the generated point cloud while it is changing its position and capturing data. The resulting point cloud is then georeferenced using this same technique. When georeferencing point clouds produced by SLAM it is important to take SLAM drift into consideration. As mentioned in Keitaanniem et al. (2023) SLAM, which uses easily identifiable points to navigate and map its

surroundings, is subject to the errors stored in these points. When these points are used as references, these errors add up and cause what is referred to as SLAM drift errors. To alleviate this issue Keitaanniem et al. (2023) proposes separating larger sections into smaller for post processing as this has proven to lessen the issue of SLAM drift. The authors also bring up the importance of the start and stop locations to be the same when measuring with a SLAM based scanner, this is known as loop closure and has been proven to lessen the misalignment in the point clouds after georeferencing.

2.2 Use of 3D laser scanners in the mining industry

Underground mining operations require highly detailed and precise surveys to maintain productivity, minimizing workplace hazards and safety as well as following the environmental aspects and regulations of the entire process. This makes for a challenging and labor-intensive industry to use laser scanners (Ellmann et al., 2021). Traditional surveying techniques are time-consuming in nature, and even if the techniques are accurate and effective for many projects, this can cause problems in an industry with large scale projects such as mines. When asked what mining companies like LKAB are requesting from surveyors, B. Fjellborg (personal communication, 4 May 2023) said that accuracy and readability of details are the key points. From the collected data, tunnels are turned into meshes to be used as the basis for the location of drill holes in which explosives are planted to expand the mine in a safe and controlled way. It is of extreme importance that these models are highly accurate and easy to read when these drill holes are planned. Scanned models will also be compared to theoretical models, to determine whether the physical tunnel has been excavated too narrowly or too wide. If either of these cases are true then this could prove highly expensive for the mining company, as there may be a need to go back and further expand a tunnel to make sure that it holds the right dimensions and allows for the passing of equipment.

Another task placed upon the surveyor is to create and georeference a 3D model of the mine. This digital model must be accurate enough so that when coordinates are extracted from the model to be used in different projects, these positions won't differ between the physical cave and the 3D model. The 3D model also has to be detailed enough and have a clear readability so that it can be displayed for various purposes, such as displaying the mine, tracking progress, risk management, maintenance and planning for further projects within the mine (B. Fjellborg, personal communication, 4 May 2023).

For such tasks, high accuracy and production efficiency cannot be compromised, which has led surveyors to 3D laser mapping over traditional surveying techniques in the mining industry. The 3D laser techniques offer advantages in both accuracy and speed and can be used without having to interrupt the productivity flow. It is possible to produce a precise map of an entire mine in the space of a few hours (Merwe & Andersen, 2012).

3D laser mapping is based around the utilization of lasers to capture spatial data. This spatial data comes in the form of several millions of points which represents the shape, position, and spatial location of physical objects. Latitude, longitude, and elevation coordinates are scanned with extremely high accuracy that is comparatively unobtainable with traditional surveying techniques. These 3D laser scanners started out as stationary devices which scanned a section at a time to build up a 360 degrees virtual representation of a mine, these individual scans then must be registered together before producing a single coherent point cloud. In recent years an even faster method has started to be utilized more by the mining industry, SLAM based 3D scanners.

Stationary laser scanners have primarily been used for single-epoch mapping in mines to detect surface characteristics and geological structure discontinuities. Static LiDAR has also been used to monitor small areas in the mining industry for potential hazards like rockfall. The primary reason for stationary laser scanners to not be applied to multi- epoch mapping and large- scale monitoring is the slow data collecting speed. This makes static LiDAR less practical for frequent mapping and monitoring applications (Singh et al., 2023).

2.2.1 SLAM based scanners in the mining industry

SLAM has brought with it drastic improvements and capabilities to the mining industry. With the possibility to map an area whilst tracking the device's location in the area it is possible to produce detailed and accurate virtual representations of mines in shorter spaces of time than compared to stationary laser scanners. This is further improved upon by combining SLAM technology with MLS devices such as handheld units, drones, and robots. This has had huge implications for the mining industry as this technology allows for unmanned mapping of potentially hazardous areas within mines and tunnels. With the increased speed and user friendliness of handheld devices it is also quicker and simpler to rescan areas to check for deformations within the area. By mounting SLAM based scanners on drones or robots it is possible to map areas inaccessible to personnel, further helping with exploration and expansion of mines without risking any human life.

As opposed to stationary laser scanning, SLAM based MLS devices also have been shown to work for multi- epoch mapping and large- scale monitoring in mines. This is primarily due to the increased data collection speed since mobile devices do not need to be set up at any specific scanning station. These types of scanners produce data with high temporal and spatial resolutions that makes them ideal for deformation monitoring (Fahle et al., 2022).

2.3 Different kinds of SLAM

SLAM was introduced as a methodology to tackle the problem of navigating and mapping terrain without good reference points or with poor access to satellite data for early autonomous robotics (Whyte & Bailey, 2006).

As mentioned in Kazerouni et al. (2015) SLAM is commonly split into two separate processes, creating the map of the surrounding area and using the information interpreted by its sensors to continuously calculate the location of the measuring device in this map. The methodology utilizes different sensors, depending on its application, to continuously determine the location of the measuring device as well as create a map of the surrounding area. Depending on its application, examples of the sensors utilized are visual sensors such as cameras, optical sensors such as light detection and ranging (LIDAR) and acoustic sensors such as microphones (Evers & Naylor, 2018). These sensors are commonly used in conjunction with one another to produce more accurate results, data from an IMU is also commonly applied.

The LIDAR SLAM (LSLAM) determines the location of its measuring device as well as, maps the environment around it, by measuring the travel time from send to receive of a light pulse with a known frequency sent from the LIDAR device. Due to the precise accuracy of the point clouds that are produced using LSLAM and the speed at which they can be created, it is commonly used in construction projects, tunnel, and cave mapping as well as guidance for autonomous robots and vehicles (Nam & Gon-Woo, 2021).

Acoustic simultaneous localization and mapping (ASLAM) uses sensors that can receive and interpret sounds, such as microphones. The sensors on the device receive waves of sound and are able to interpret the direction of arrival (DOA) as well as the magnitude of the waves. As mentioned in Evers and Naylor (2018) ASLAM can deduce these inputs and representing where the sources of sound originate from by creating a 3D map. The authors conclude that the method, although successful in mapping and localizing the device, the results are susceptible

to degradation when tasked with mapping several sources of sound at once (Evers & Naylor, 2018).

Visual SLAM (VSLAM) utilizes visual sensors like cameras to map their surroundings and continuously determine the location of the device. As mentioned in Tourani et al. (2022) the use of visual sensors as opposed to optical sensors is cheaper, lighter and can represent the colors in the surroundings more accurately. In the article it is mentioned that this type of SLAM struggles when there are limited sources of light and therefore VSLAM is commonly used in conjunction with other sensors like LIDAR and IMU (Tourani et al., 2022).

2.3.1 SLAM with LIDAR incorporated WILDCAT

WILDCAT is a 3D LiDAR- inertial SLAM system with high accuracy and robustness designed for autonomous systems, localisation, mobile mapping and mapping in real- time. The system allows for high-accuracy mapping and positioning by devices in complex and challenging environments, all without needing access to GPS or any other external positioning information.

WILDCAT combines a real- time LiDAR- inertial odometry module which utilizes a continuous time trajectory representation, with a pose- graph optimization module. The optimization module supports both single- and multi- agent settings which makes the WILDCAT system highly versatile, modular and reconfigurable as well as easy to integrate (Ramezani et al., 2022). This was demonstrated at the Defense Advanced Research Projects Agency (DARPA) Subterranean Challenge where the WILDCAT system outperformed other SLAM based systems in various types of sensory- depriving and challenging environments (Ebadi et al., 2022)

2.4 HMK regulations

To assess the quality of a 3D mapping and localization project there are several parameters which can be analyzed throughout the project to maintain an acceptable level of uncertainty. There also exists four different HMK- standard levels as defined in HMK- Geodatakvalitet. (2017) which acts as recommendations for the client's choice of method and the kind of parameters they wish the surveyor to follow. The standard levels range from zero to three, where zero has the lowest demand for data quality. Depending on what standard level the client wants the project to follow, also determines how the project is carried out in certain stages.

HMK- standard level three is used in project planning and construction of infrastructures and buildings since it has the highest demand for accuracy and geometric resolution. The document specifies that the maximum allowed accuracy

for a HMK- standard level three project may not exceed five centimeters (HMK-Geodatakvalitet, 2017). Terrestrial laser scanners fall in the category of geodetic measuring methods that can capture data and maintain these high demands of accuracy and as such HMK standard level three is used for terrestrial laser scanner projects.

In the document HMK- Terrester laserskanning, (2021) the demands for a laser scanning project that follows HMK- standard level three are listed and distinctions are made between accuracy, absolute- and relative accuracy. Relative accuracy is applied to TLS data which has not been georeferenced to a global reference system and is instead georeferenced to a local reference system. Absolute accuracy refers to TLS data which has been georeferenced to a global reference system like SWEREF99. The accuracy depends on the type of instrument and is specified in the statistics of the device. The document also specifies that the minimum point density in the point cloud is regulated by the demands as specified by the client, depending on what level of object detail is required (HMK- Terrester laserskanning, 2021).

HMK- Terrester laserskanning, (2021) states that the best way to verify the relative accuracy of a georeference point cloud is by using checkpoints. These points are marked by signals or targets and have known coordinates, after georeferencing the point cloud the coordinates for these checkpoints are compared to the previously known coordinates. By calculating the root mean square (RMS) for plane and elevation, a value is given which shows the average error between the georeferenced point cloud and the reference system. According to HMK- standard level three the relative accuracy of a georeferenced point cloud should not be larger than five millimeters in regard to planar- and elevation coordinates. The 3D RMS- value for the point cloud can be calculated by combining planar and elevation data which becomes relevant for registering and georeferencing point clouds. The relative accuracy demands for the 3D RMS- value is typically specified by the client.

3 Methodology

The case study is conducted by processing data by registering and georeferencing point clouds. Further processing is then conducted by calculating volumes of meshes produced from the point clouds and comparing these to each other as well as a theoretical volume. An overview of the workflow for this case study can be found in figure 1.

3.1 Software and materials:

Software:

- SBG GEO version 2023.1.3.332
- Faro Scene version 2023.0.1.10677
- Autodesk AutoCAD Map 3D 2023 version 26.0.37.2
- CloudCompare version 2.13
- Poisson Surface Reconstruction plugin by Mizha Kazhdan for CloudCompare

Materials:

- Materials used for this project consist of laser scanned data provided by Blå Projekt, Process & GIS AB.
- Raw scan data gathered in a tunnel using Faro Laser Scanner Focus 3D X 330
- Raw scan data gathered in a tunnel using EMESENT Hovermap HF1
- Coordinate files for reference points within two tunnels

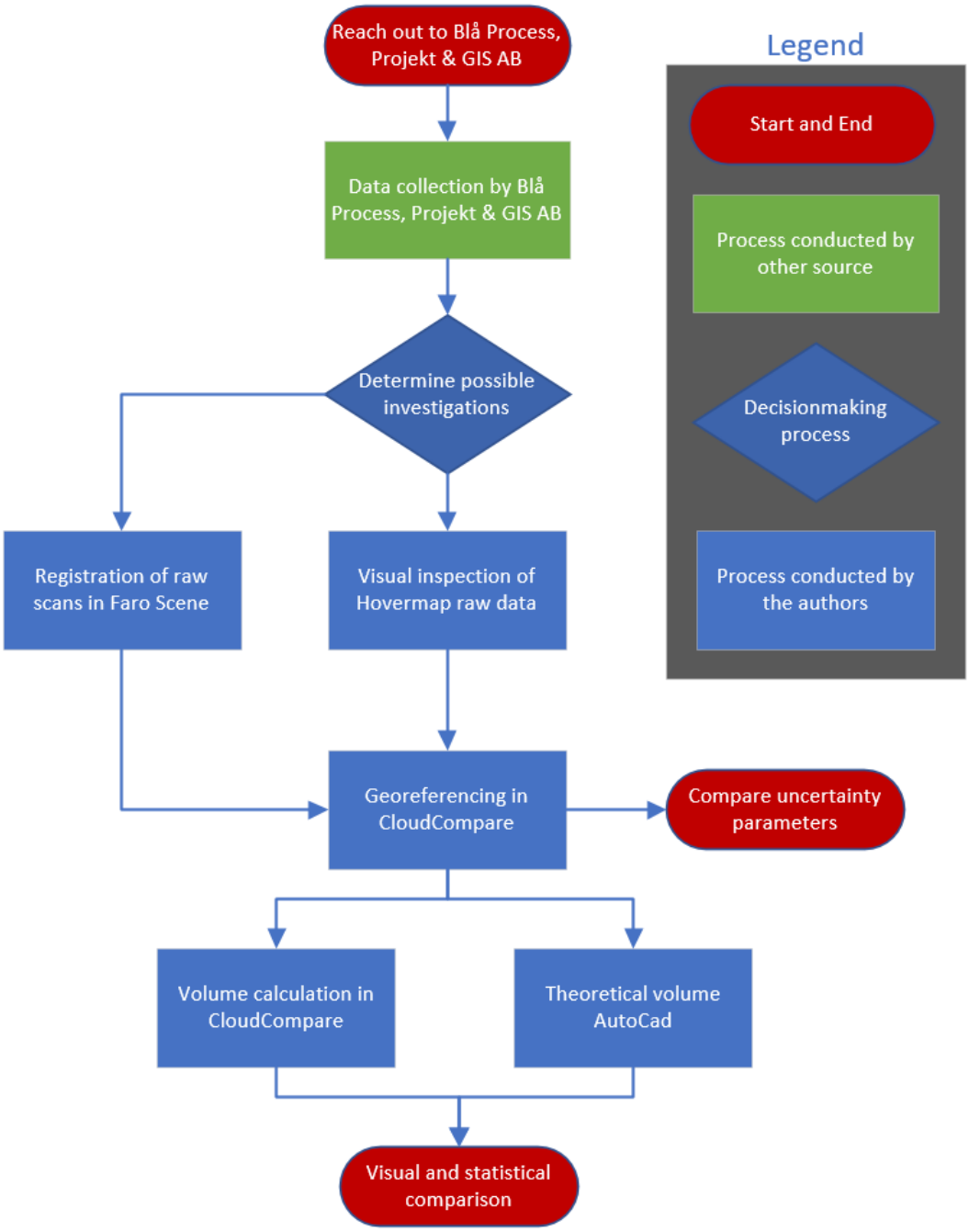

Figure 1. Workflow describing an overview of what was done in the project.

3.2 Instruments

The Faro Laser Scanner Focus 3D X 330 is a high- speed 3D terrestrial laser scanner that is capable of recording 976 000 single point measurements per second at a maximum range of 330 meters (see appendix A). The implemented phase shift technology means that constant waves of infrared light are projected outwards from the scanner. These waves are of varying length and upon being reflected to the scanner the phase shifts in the waves accurately determine the distance between the object and the scanner. The Faro scanner is equipped with class one laser that has

beam divergence of 0.19 milliradian and an exit diameter of 2.25 millimeters. The scanner has an LiDAR accuracy error of two millimeters (FARO, 2015).

The Emesent Hovermap is a SLAM based mobile laser scanner capable of recording 300 000 points per second at a maximum range of 100 meters (see appendix A). The Emesent Hovermap is equipped with a WILDCAT SLAM solution, Emesent autonomy algorithms and the Emesent Aura. All these systems aim to improve the capabilities of the device in challenging GPS- denied environments. The Hovermap MLS is equipped with a class one laser and has a LiDAR accuracy error of 15 millimeters in underground environments. The device can be deployed handheld as well as mounted on drones, vehicles, backpacks, or ground robots. (EMESENT, 2022).

3.3 Study Area

The study area is situated in the north of Sweden several hundred meters below a town called Kiruna. The area is part of a large tunnel system within the Kiruna mine which is an active mine exploited currently by LKAB for its precious metals and minerals. The area of interest for this study is a section of the mine that's roughly 210 m long in a curved shape. It's an interesting area as the curve brings further challenges for both methods of laser scanning which may not exist in straight tunnels. The area was scanned by an external company called BLÅ Projekt, Process & GIS AB with two different laser scanners: a stationary TLS and a handheld SLAM based MLS. Within the tunnel several reference points have been placed on the tunnel wall, each of these reference points are marked with a small sphere placed inside a larger triangle painted onto the tunnel wall. Under each marking is a number to indicate which reference point it is and a map was provided, showing the location of each reference point and its number in the tunnel (see appendix B).

The study area's location is presented with the help of the software GEO in figure 2. In the figure the area is represented by a pink mesh at the bottom left of the figure and the unit in the coordinate system is meters. The various dots are reference points in the local coordinate system. Elevation is calculated from the top of Kiirunavaara which is a mountain located in Kiruna in which the Kiruna mine is located, hence these coordinates are not below sea level but rather calculated as distance below the peak of Kiirunavaara.

The mining tunnel is roughly 210 m in walking distance from end to end, roughly 5.2 m floor to ceiling and roughly 7 m side to side.

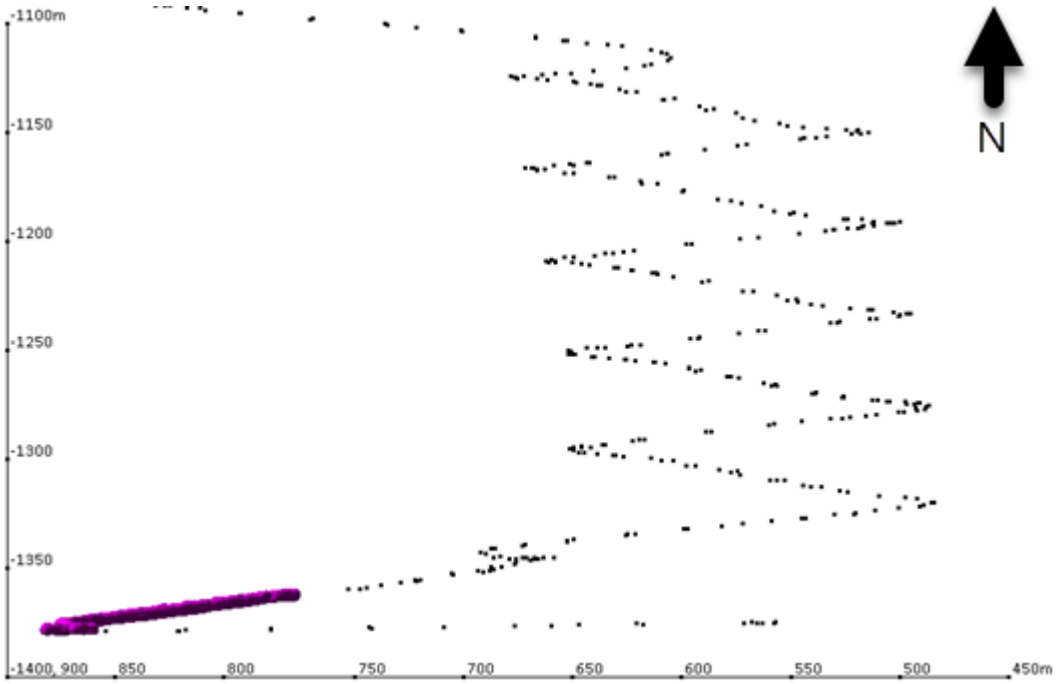

Figure 2. Shows the location of the study area. The pink mesh in the bottom left of the figure represents the study area and the points represent reference points. The scale is in meters.

3.4 Data collection by Blå Projekt, Process & GIS AB

To source data the authors, with the help of their supervisor, reached out to Blå Projekt, Process & GIS AB as they were in the process of mapping parts of the Kiruna mine using laser scanners. All data used for this project was gathered by Blå Projekt, Process & GIS AB inside the Kiruna mine in Kiruna Sweden. The raw data was transferred to Gävle for further processing. The data was collected on the 19th of March 2023 deep in the Kiruna mine using the TLS Faro Laser Scanner Focus 3D X 330 and on the 20th of March 2023 using the MLS Emesent Hovermap. Inside the mine exists an established reference system marked with reference points that are located on the tunnel walls. A total of 19 reference points exist in the section of the tunnel, out of these 17 were used for the project as the supplied data did not contain coordinates for all 19. The coordinates for the reference points can be seen in table 1 and are displayed in the local reference system used within the mine. The X-axis in this reference system grows towards the east as opposed to the west and the Y-axis grows towards the south rather than the north. This is because the reference system used in the mine follows the excavated ore vein and uses the peak of Kiirunavaara mountain as the zero point for its elevation which results in negative elevation values.

Table 1. The reference X, Y and Z coordinates are presented in the Kiruna mine's local coordinate system, the unit is meters.

Point ID	Reference X, Y, Z coordinates (m)		
40261	791.385	6135.560	-1363.720
40262	818.382	6149.440	-1367.420
40263	842.848	6147.770	-1370.260
40264	866.207	6152.780	-1373.900
40265	868.525	6161.500	-1374.460
40266	881.140	6157.320	-1375.060
40267	879.254	6168.700	-1375.950
40268	896.454	6182.750	-1377.240
40269	888.824	6185.860	-1377.150
40271	894.820	6200.290	-1377.880
40272	892.417	6216.170	-1378.720
40273	889.568	6234.460	-1379.130
40274	878.454	6246.190	-1379.480
40275	886.826	6253.060	-1379.450
40277	889.281	6263.860	-1378.980
40278	885.094	6263.235	-1379.366
40279	874.687	6260.232	-1378.577

For the purpose of laser scanning this tunnel, Blå Projekt, process & GIS AB used white spheres with known radii, these were placed on tripod stands and their coordinates were measured using a total station. These spheres can then be used in the processing stage, with input from the user regarding the radii and location of the spheres, the software can automatically register the point clouds from the Faro TLS. Spheres on the reference points on the walls were also placed during the scans such that they could be easily identified during the georeferencing stage.

The exact amount of time required to establish the spheres on tripods is not known. According to B, Fjellborg (Personal communication, 4 May 2023) they estimated setting up the Faro TLS and doing a full dome scan took around 6 minutes per station. As this section of the tunnel required 12 stations, the time spent laser scanning this section is approximately 72 minutes. In contrast to the data collection

conducted with the Hovermap which according to B, Fjellborg (Personal communication, 4 May 2023) took around 15 minutes for a full walkthrough of the area and did not require establishing spheres on tripods but rather used the established reference points on the walls as easily identifiable points for its SLAM algorithms.

3.5 Initial data processing

The amount of time required for the pre-processing of the Faro raw data scans and the Hovermap raw data scans differs. Since raw scans were requested for this project, the raw scans produced using the Faro laser scanner required two steps of processing, registering and georeferencing while the Hovermap which uses SLAM algorithms creates one big point cloud for the entire tunnel. As such, more work is required to process the Faro TLS scans. Registering point clouds is the process of fusing multiple point clouds into one spanning the entire area and transforming it to fit into one of the raw scans coordinate systems. Georeferencing can be done at the same time as the registering via direct georeferencing or after the point cloud is registered via indirect georeferencing. Both methods seek to transform the coordinates to an outer coordinate system, in the case of this project the coordinates are transformed to fit Kiruna mine's local coordinate system.

3.5.1 Faro Laser Scanner Focus 3D X 330 data processing

As the raw files came from a Faro laser scanner they had to be opened and initialized using Scene software. In the software the individual raw scans were first processed individually to allow the software to detect target spheres for registration. The processed scans were then registered by importing coordinates of known, easily identifiable spheres with known radii. With this input from the user, the software is able to automatically register the individual raw scans into one complete point cloud for the entire tunnel. The chosen process for automatically registering the scans is target based which means it utilizes the description of the targets that the user input to determine how to correctly fuse the scans together. The software identifies the spheres locations in one stations raw scans and then identifies it again in the next scan, this information is then used to register the scans together Target based registration was chosen over the likes of cloud to cloud registration as the cloud overlap in the data set was not deemed sufficient, around 25 %, and target based registration has the advantage that the accuracy of the registration easily can be verified. Although previous studies have shown promising results when using complex algorithms to register point clouds with low overlap together as in Liu et al. (2021), this was not deemed achievable to learn and produce in the allotted time of this project. As mentioned in HMK-Terrester laserskanning (2021) the automatic process of target-based registration cannot be fully trusted and as such the targets

that were identified by the software were always visually verified to be correct by the user and the point cloud was also inspected. As the raw files were delivered without being registered together, it was determined that fusing the individual scans into one point cloud and using the method of indirect georeferencing. Within the point cloud there were identifiable targets with well-established coordinates in the local coordinate system that could be used in the registration process. The quality of the registration produced in Faro Scene can be seen in table 2. As target-based registration was used, parameters such as point cloud overlap are not available. The registered point cloud was then exported in e57 format to preserve its parameters and imported into the CloudCompare software for georeferencing to the Kiruna mine's local coordinate system.

3.5.2 Emesent Hovermap data processing

The raw scan files from the Emesent Hovermap did not require pre-processing in the form of registration to create a point cloud as this had already been done by the Hovermap and its SLAM algorithms. As such the raw scan files were imported directly into CloudCompare and inspected visually before being georeferenced to the Kiruna mine's local coordinate system using the coordinates of the reference points. The point cloud generated by the Hovermap MLS and the point cloud from the Faro TLS can be seen in appendix C presented in the CloudCompare software.

3.6 Georeferencing the point clouds

As mentioned by Rakotosaona et al. (2019) point clouds produced by laser scanning are often subject to noise in some form. Therefore, before georeferencing both point clouds were run through a low pass noise filter which cleans up the point clouds using a form of nearest neighbour interpolation that takes into consideration the nearest 8 neighbours of each point and only leaves the desired points. The georeferencing required similar steps for both point clouds. The reference points in table 2 as well as the point clouds were imported to the software CloudCompare. To ensure only reference points that had proper scan coverage from both laser scanners were used, the point clouds from the Faro laser scanner and the Hovermap were segmented to be the same size. By using the segmenting tool in CloudCompare, the roof of the tunnel was removed in both point clouds to allow clear visibility of the reference points. Using the align tool in the software the point cloud was aligned and transformed to fit the local reference system of the mine. The RMS values were then calculated using the formula found in HMK- Terrester laserskanning (2021). Where $\Delta X_i^2, \Delta Y_i^2$ and ΔZ_i^2 are the coordinate deviation between the georeferenced reference point coordinates and the know reference point coordinates, and n is the total number of used reference points (see equation 1- 3).

Equation (1)

$$RMS_{höjd} = \sqrt{\frac{\sum_{i=1}^{n} \Delta Z_i^2}{n}}$$

Equation (2)

$$RMS_{plan} = \sqrt{\frac{\sum_{i=1}^{n} \Delta X_i^2 + \sum_{i=1}^{n} \Delta Y_i^2}{n}}$$

Equation (3)

$$RMS_{3D} = \sqrt{\frac{\sum_{i=1}^{n} \Delta X_i^2 + \sum_{i=1}^{n} \Delta Y_i^2 + \sum_{i=1}^{n} \Delta Z_i^2}{n}}$$

3.7 Visual inspection

The visual inspection of the point clouds was carried out largely in CloudCompare and follows the guidelines in HMK-Terrester Laserskanning (2021) for visually inspecting the point cloud. However, some visual inspection was carried out in AutoCad Map 3D for the theoretical volume model. A parameter that was of interest for the project was visual clarity, how easily identifiable check points were and the legibility of text. This was inspected by creating cut-out sections of the same area and visually comparing the legibility of text and if the laser scanners had hit the spheres with an adequate number of points such that they were easily identifiable for the user and the software. Being able to correctly identify spheres used for georeferencing and registering plays a large role in getting a good result as can be seen in the differences in RMS values for points with good coverage and bad. For this task, the reference points 40279 which can be seen in figure 9 and 40262 which can be seen in figure 10 and 11, were chosen. Reference point 40279 is located right above a sign with the text “Norr” while reference point 40262 is a good representation of the average reference point in the mine with the only visual distinction being the sphere itself and the numbered triangle surrounding it.

As the final step, the two georeferenced point clouds were imported at the same time to look for any visual differences or deformations which would in theory become visible once the point clouds were directly placed on top of each other as they were both georeferenced to the same coordinates.

3.8 Volume calculation

The volume of a point cloud can be calculated using different methods. One approach is using the method proposed by Zhi et al. (2016); it proposes fitting the point cloud to a projection plane and taking cross sections with set distances between them and then calculating the area and volume. However, this is a time-consuming process with a point cloud of this size and for this reason the volume calculation for this project was carried out in the software CloudCompare where the software does most of the work. After both point clouds had been georeferenced such that they were transformed and aligned to overlap, they were segmented with straight angles in the same places to keep them the same size. As the hardware requirements to process a point cloud of this size were too large, the point clouds were subsampled to contain fewer points. As point clouds are not solids and often contain holes where scanners don't get good enough covers, the first step was to create a mesh that would represent each point cloud. This was done by calculating the normals of each point cloud and using a plugin called Poisson Surface Reconstruction made by Mizha Kazhdan. The plugin is based on solving a 3D Laplace equation as described in Kahzdan et al. (2006). The plugin creates a triangle-mesh based on the orientation of the points in the point cloud. The mesh that is produced has no holes and is watertight, even if the base point cloud is not, which makes it possible to calculate its volume. Figures 14 and 15 present the produced mesh for the Faro TLS and the Emesent Hovermap MLS in the CloudCompare software.

To have some sort of reference to what the correct volume of the tunnel should be, a theoretical model of the tunnel, which depicts what the mining company intends to excavate, was acquired. The theoretical tunnel was processed in AutoCad and a cross section can be seen in figure 17.

4 Results

4.1 Registration of Faro scans

The twelve Faro scans were imported in the Scene software and registered using the automatic target-based method which resulted in a coherent point cloud (see Figure 3). The error values of the registered point cloud are displayed in Table 2. The unsegmented registered Faro point cloud and the unsegmented Hovermap point cloud opened in the CloudCompare software can be seen in appendix C.

Table 2. The errors from the registration of the raw Faro scans.

Parameter (mm)	Max Distance error	Mean Distance error	Max Horizontal error	Mean Horizontal error	Max Vertical error	Mean Vertical Error
Focus 3Dx 330	6.5	3.5	6.2	3.2	3.2	1.1

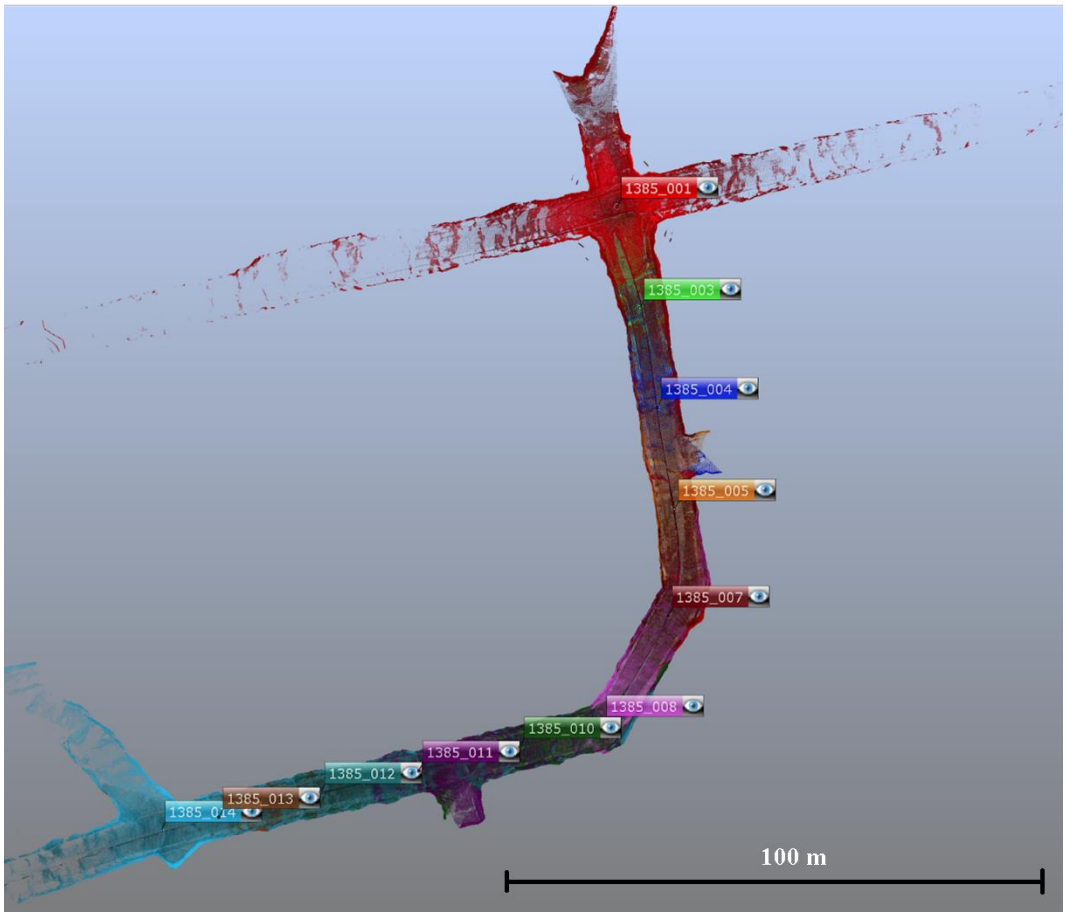

Figure 3. Registered Faro point cloud with individual scans color-coded, displayed in SCENE. The scale is in meters.

4.2 Geoprocessing point clouds

The segmented Faro point cloud and segmented Hovermap point cloud can both be seen in appendix E. After performing the georeferencing step for each point cloud, the reference points were visible within the point clouds as can be seen in figure 6 (Faro) and figure 7 (Hovermap). As for the overall points and the density of the points that are in the point clouds of the same size produced by the two laser scanners, the Faro TLS contains around 234 million points while the Emesent Hovermap MLS contains around 153 million points.

The RMS plane, RMS elevation and RMS 3D values are presented in table 3. Coordinates of the georeferenced points as well as the deviations from the reference points are presented in appendix D. These can be compared to the "true" reference points, that were measured using a totalstation and thus believed to be "true". In figures 4 and 5 the coordinate deviations from the reference points are presented and the largest deviation is labelled with its deviation. The figures show that the values in the Y-axis differ most from their reference in the Faro point cloud while the values in the X-axis differ most in the Hovermap point cloud. A visualization of how the two produced clouds differ can be found in figure 8 with a legend.

Table 3. Shows the errors from the georeferencing for both Emesent Hovermap MLS and Faro Laser Scanner Focus 3D X 330 TLS, the unit is millimeters.

Parameters (mm)	Faro Laser Scanner Focus 3D X 330 TLS	Emesent Hovermap HF1 MLS
RMS plane	4.89	21.47
RMS elevation	3.23	7.99
RMS 3D	5.86	22.91
Mean distance difference between point clouds	23.07	
Standard deviation between point clouds	38.89	

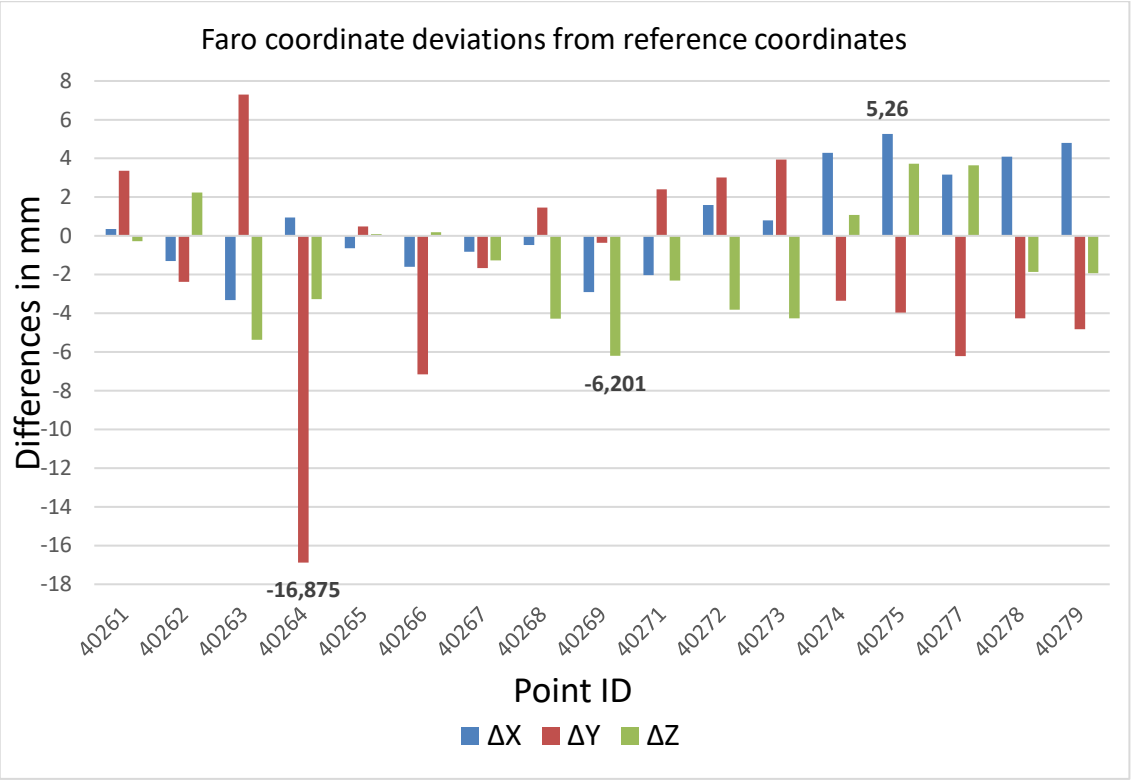

Figure 4. Coordinate differences for the Faro point cloud compared to the reference points. Differences in x, y and z-axis are presented using blue, red and green. The largest deviations for each axis are labelled with their deviation. The vertical axis unit is mm.

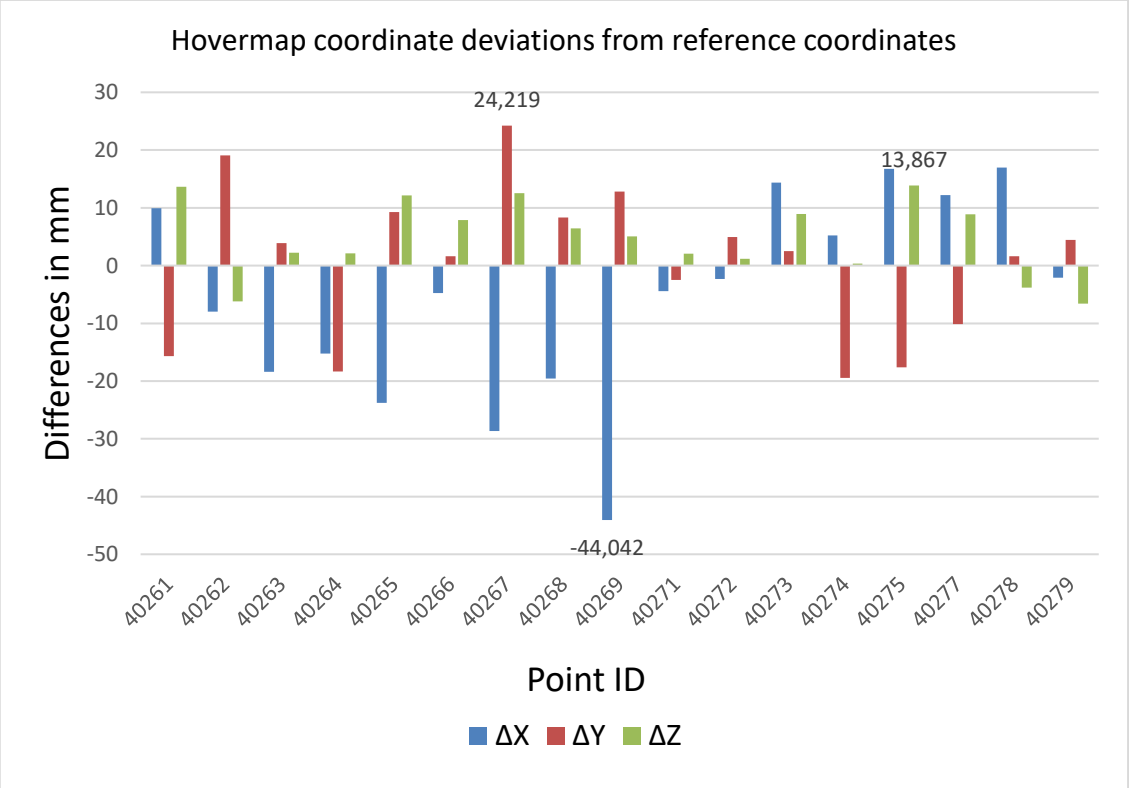

Figure 5. Coordinate differences for the Hovermap point cloud compared to the reference points. Differences in x, y and z-axis are presented using blue, red and green. The largest deviations for each axis are labelled with their deviation. The vertical axis unit is mm.

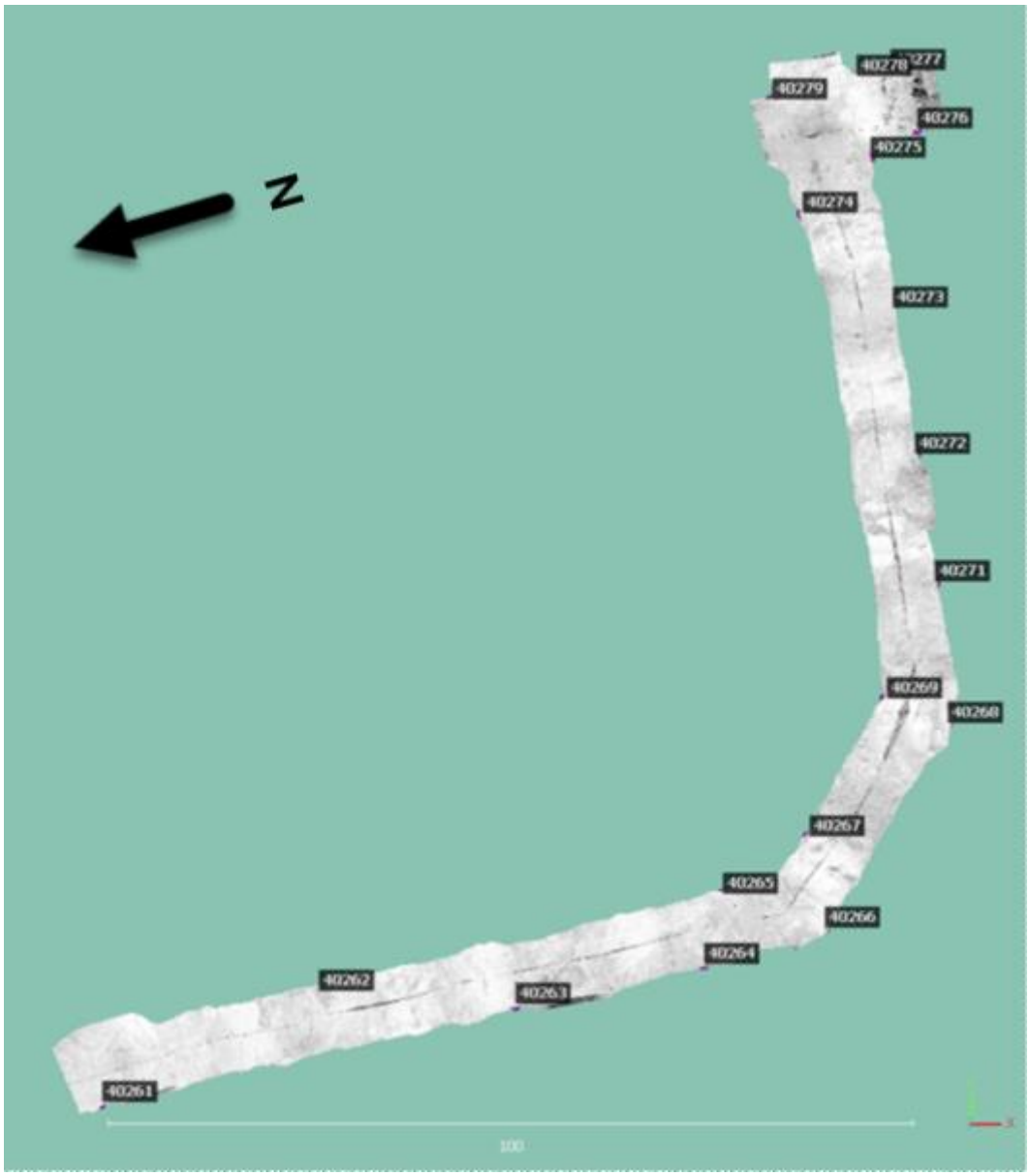

Figure 6. The segmented and georeferenced point cloud produced using faro with the reference points visible. The scale is in meters.

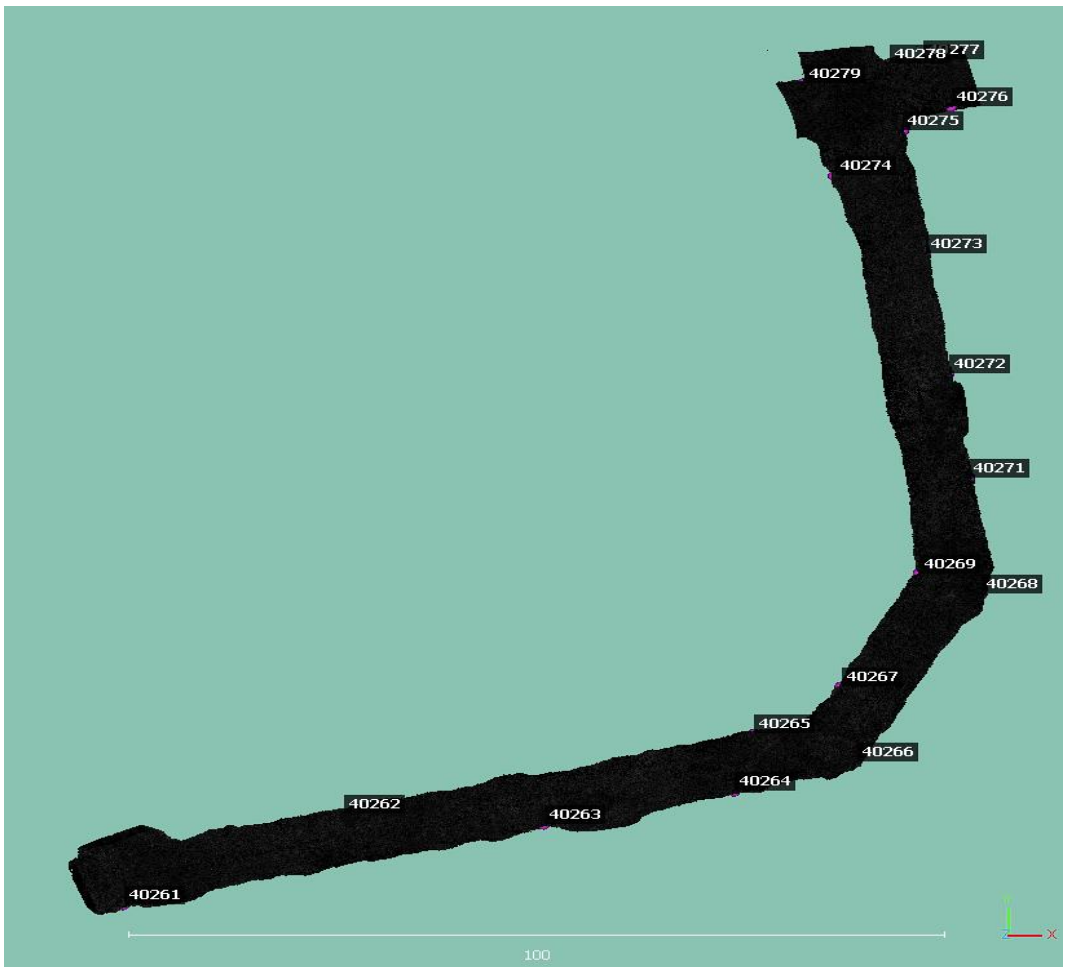

Figure 7. The segmented and georeferenced point cloud using Emesent Hovermap with the reference points visible. The scale is in meters.

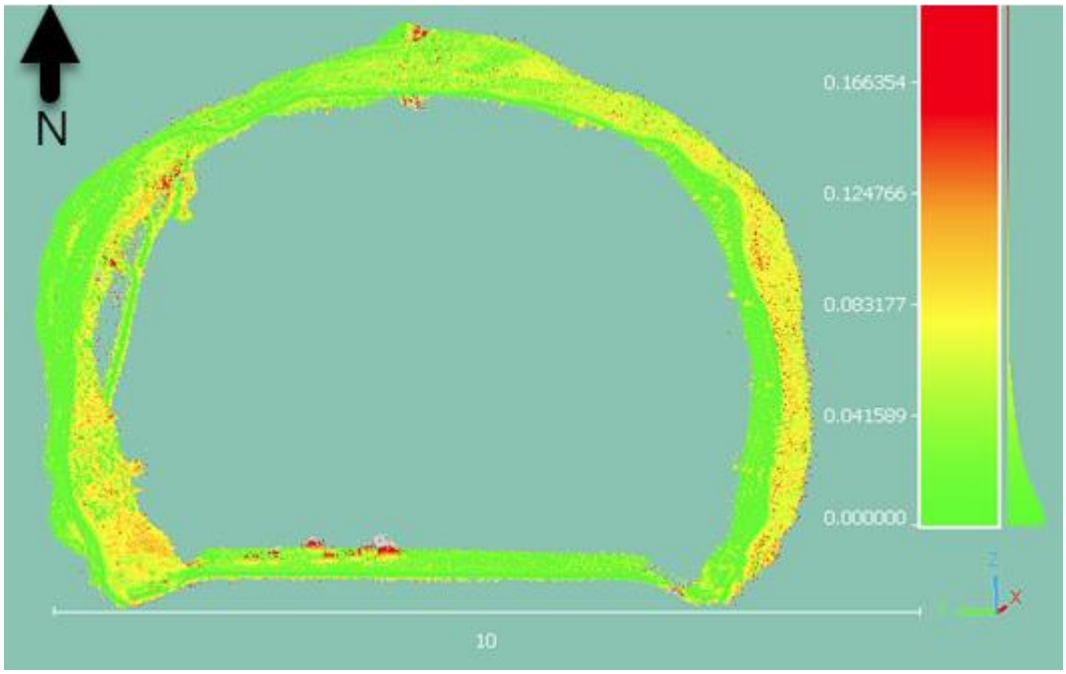

Figure 8. Distances between points in Faro and Emesent Hovermap point clouds. Green signifies smaller deviations and red signifies larger deviations. The scale is in meters.

4.3 Point cloud quality visual inspection

The quality of the reference point 40279 is compared in figure 9 a and b, the figures were captured from roughly equal distance to compare the laser scanners capabilities of visualizing signs in the mine as well as the sphere over the reference point. The comparison between reference point 40262 is seen in figure 10 (Faro) and figure 11 (Hovermap). Figure 12 displays both georeferenced point clouds imported at the same time and color coded, the Hovermap point cloud being displayed in black points and the Faro point cloud in white.
Some areas in the Faro point cloud had a much lower point density due to either the distance from the scanner position or objects obstructing the emitted laser pulses. This is clearly visible in figure 13 where a total station is obstructing the Faro laser scanner, resulting in what is called a blind spot on the tunnel wall behind the total station (Singh et al., 2023).

A cross section was extracted from the two georeferenced point clouds, covering the same area, to visualize the difference in point density between the point clouds. These can be seen in appendix F.

a) *b)*

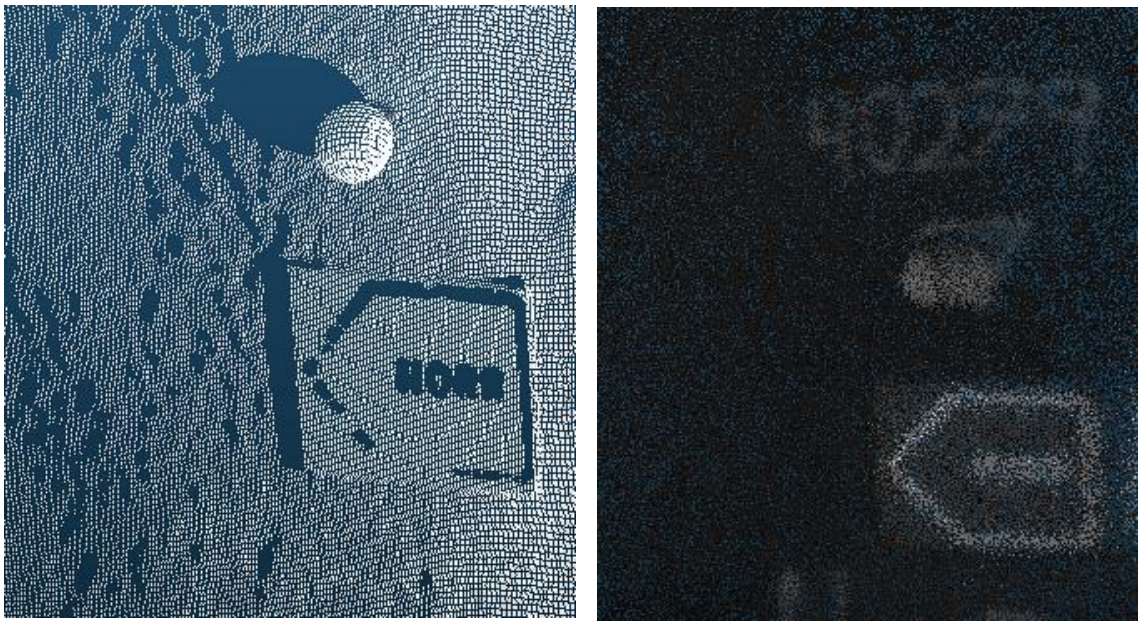

Figure 9. Figure (a) shows the reference point 40279 in the Faro point cloud. Figure (b) shows the reference point 40279 in the Hovermap point cloud. The sign in the figure says "Norr" which can be seen in figure a but not figure b.

Figure 10. Shows a poorly scanned sphere inside a red circle for clarity in the point cloud produced using Faro TLS.

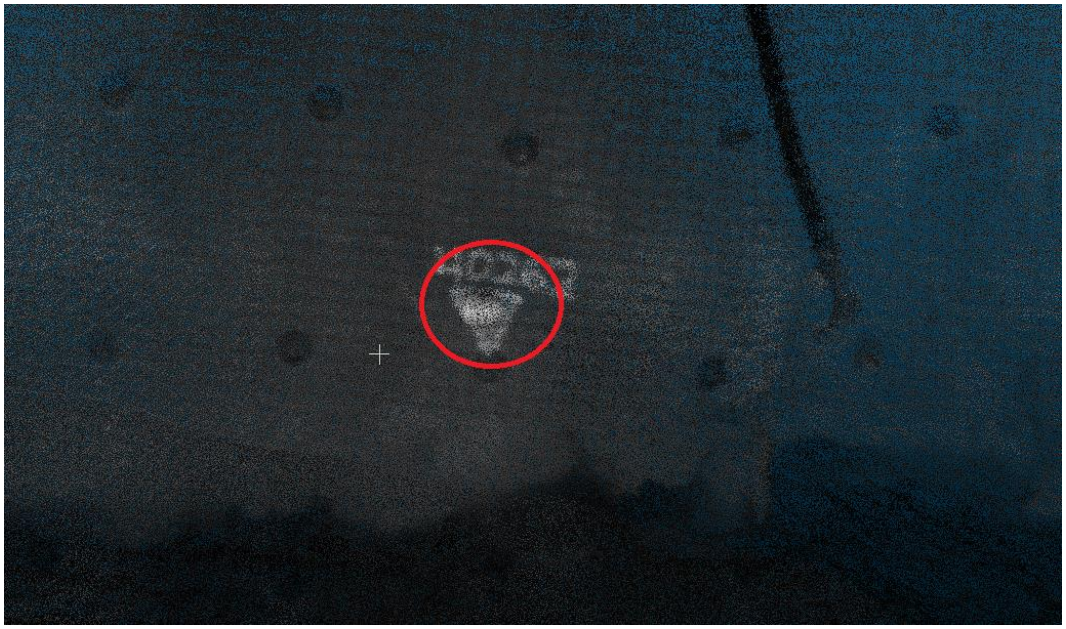

Figure 11. Shows the same sphere as in figure 9 but in the point cloud produced using Emesent Hovermap MLS.

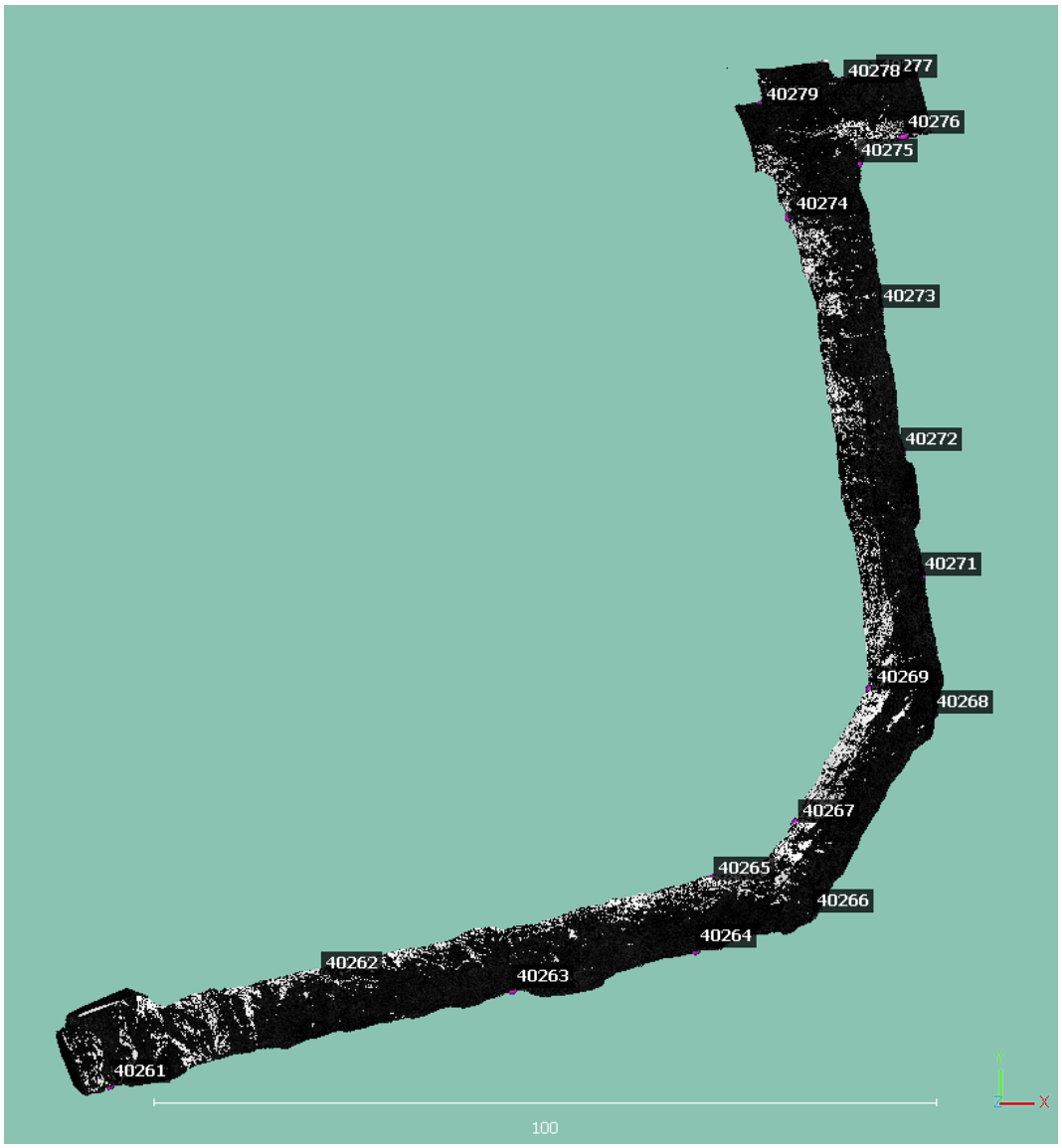

Figure 12. Shows the two segmented and georeferenced point clouds placed on top of each other. The black points represent Emesent Hovermap MLS and the white points represent Faro TLS. The scale is in meters.

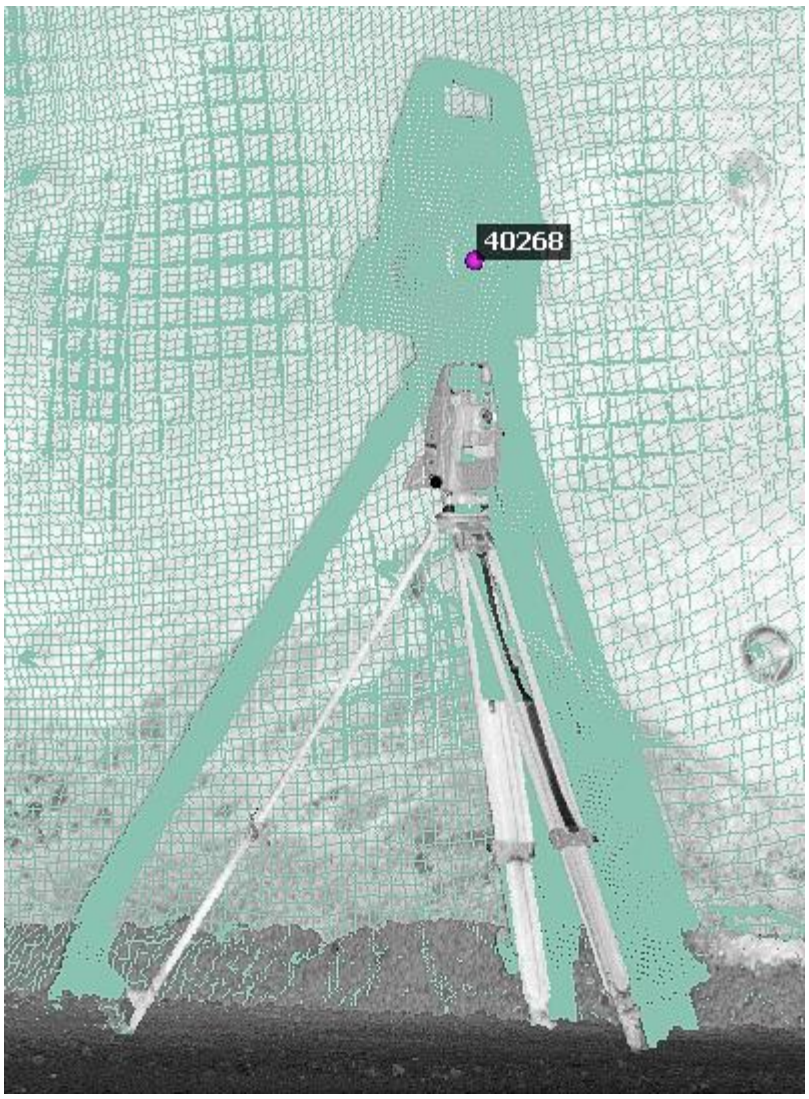

Figure 13. Shows the sphere being obstructed by a total station placed in between it and the laser scanner.

4.4 Calculated volumes

The watertight meshes produced for the Faro and Emesent Hovermap cloud points are presented in figures 14 and 15 as well as a figure presenting how the two meshes overlap in figure 16. A cross section of the theoretical model is shown in figure 17 and in figure 18 a cross section of the Faro watertight mesh has been placed on top of the theoretical model to display the comparative size between the mesh and the theoretical model.
The volume calculation for the Faro, Emesent Hovermap and the theoretical tunnel are presented in table 4.

Table 4. Shows the calculated volumes for the Faro TLS, Emesent Hovermap and theoretical model. The unit is cubic meters.

Parameter	Faro Laser Scanner 3Dx 330	Emesent Hovermap HF1	Theoretical model
Volume (m^3)	9928.07	9829.66	7489.32

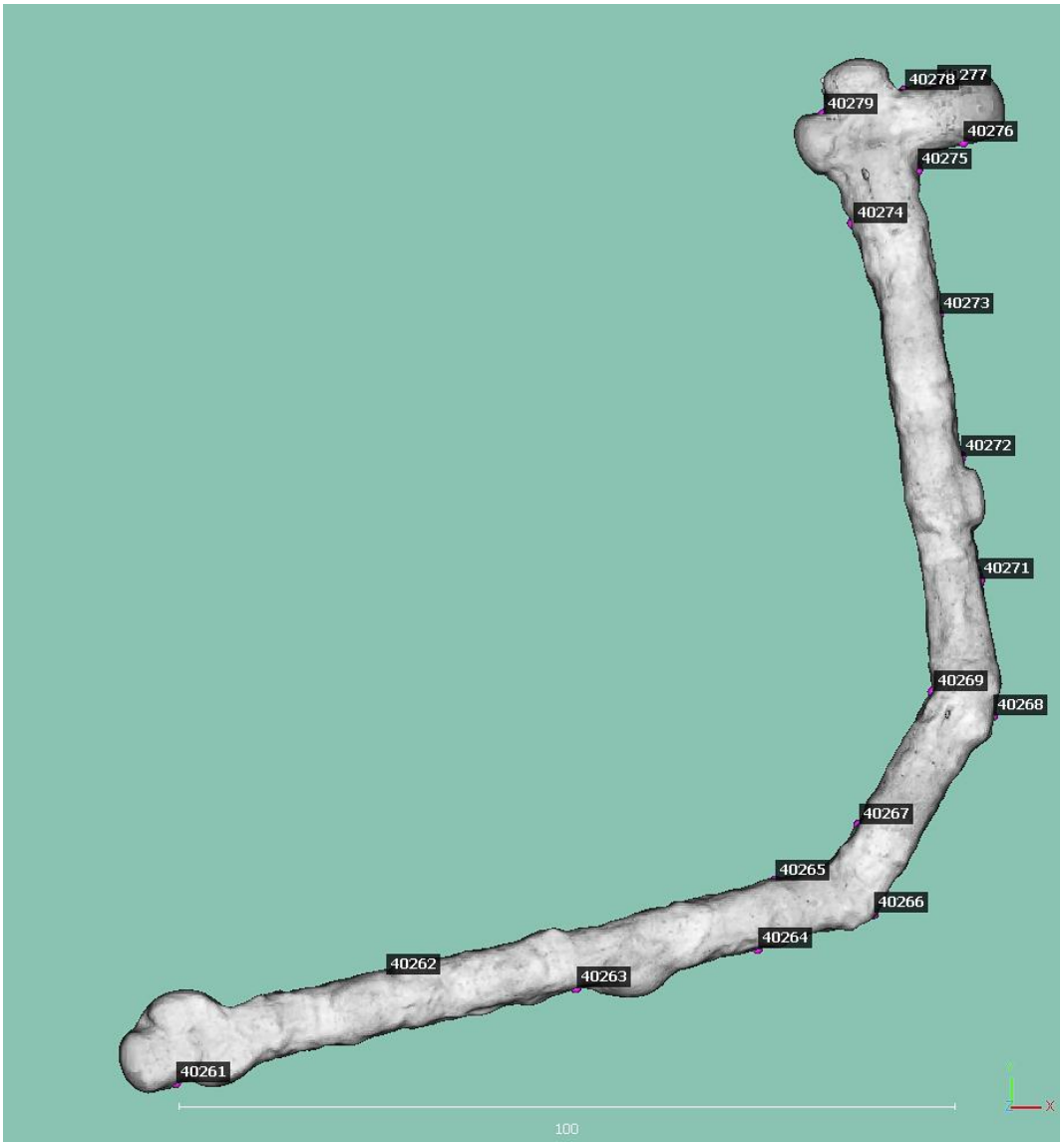

Figure 14. Shows the mesh produced for volume calculation on the Faro TLS point cloud. The scale is in meters.

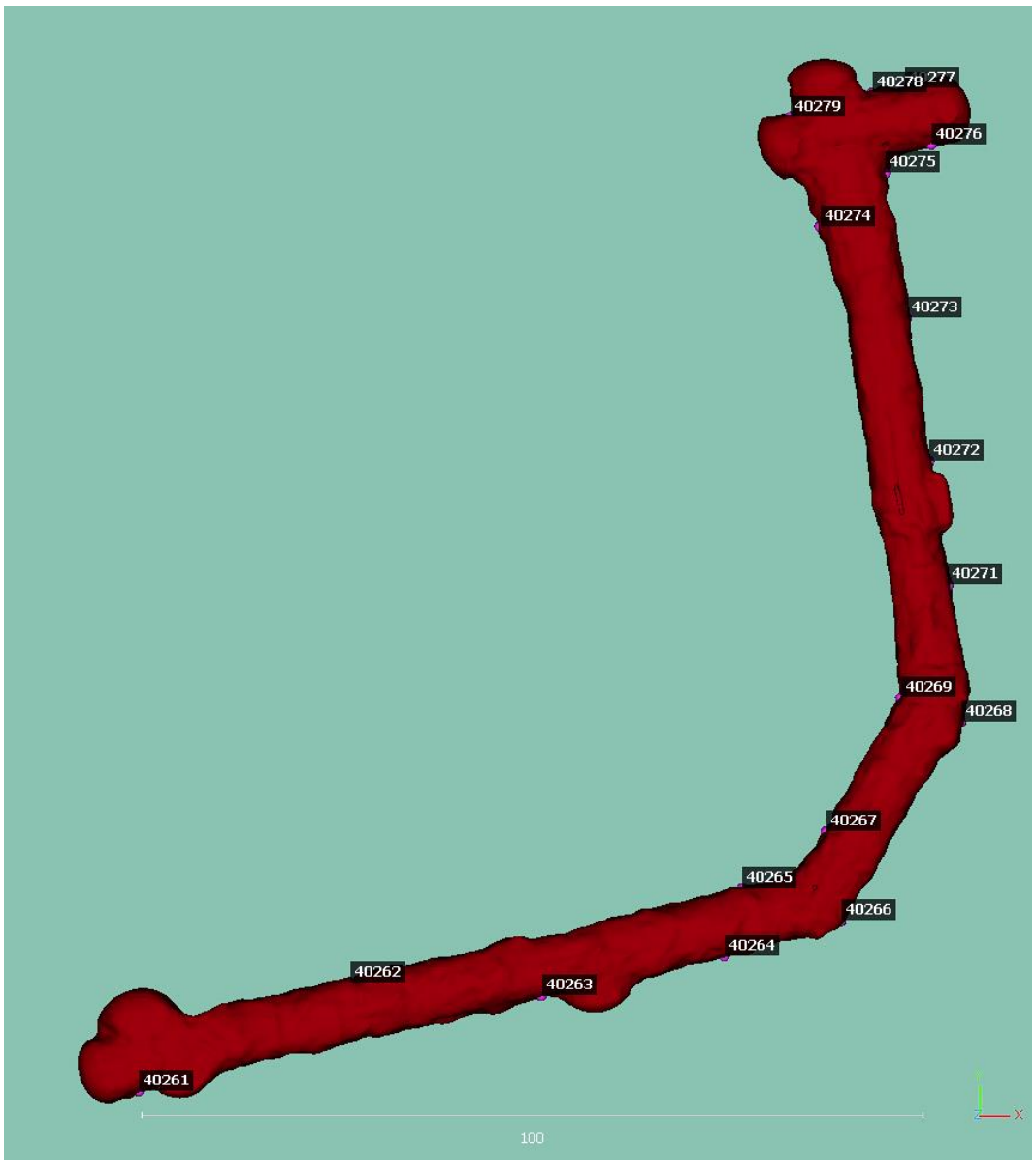

Figure 15. Shows the mesh produced for volume calculation on the Emesent Hovermap MLS point cloud. The scale is in meters.

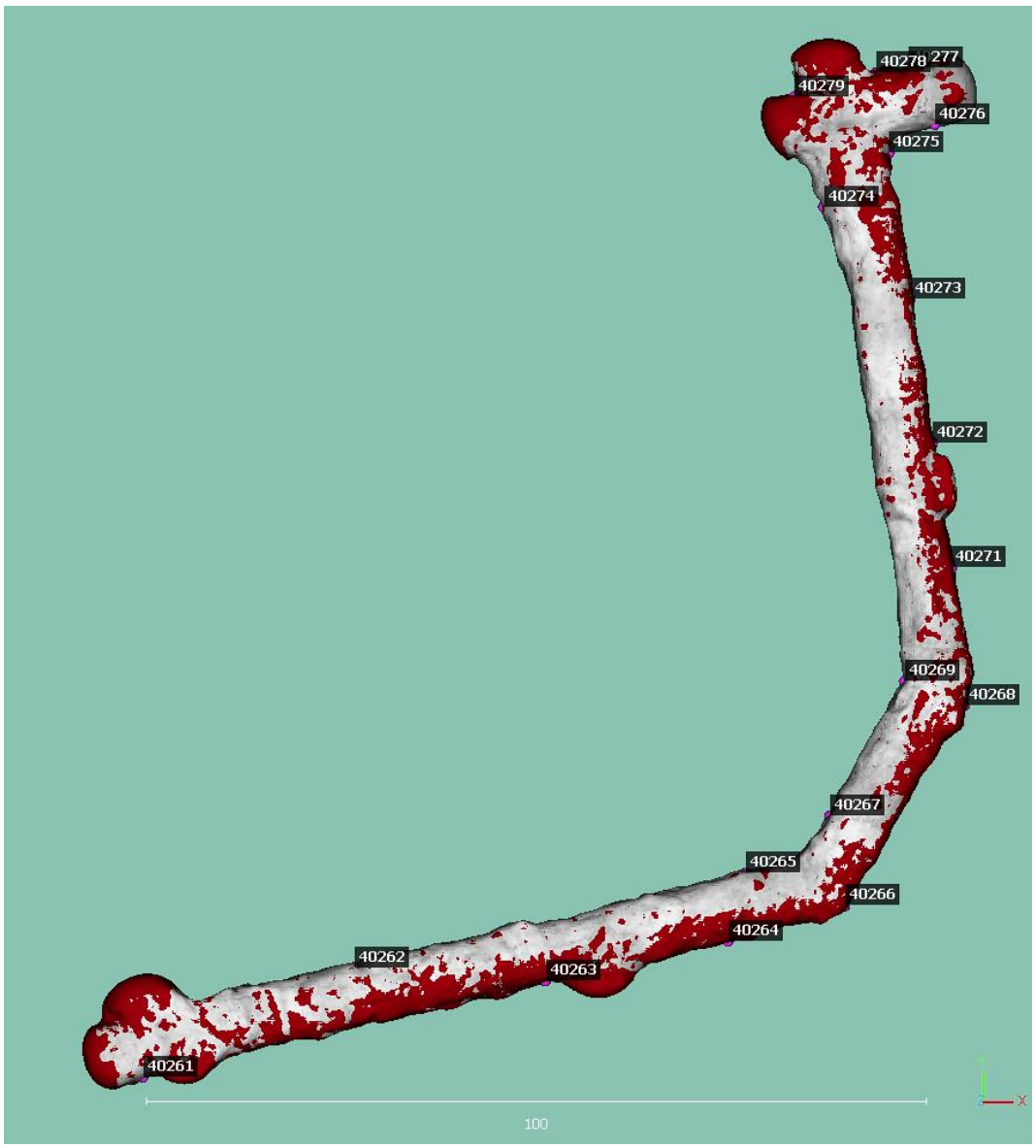

Figure 16. Shows the two meshes produced placed on top of each other. The grey represents the Faro TLS mesh and the red represents the Emesent Hovermap MLS mesh. The scale is in meters.

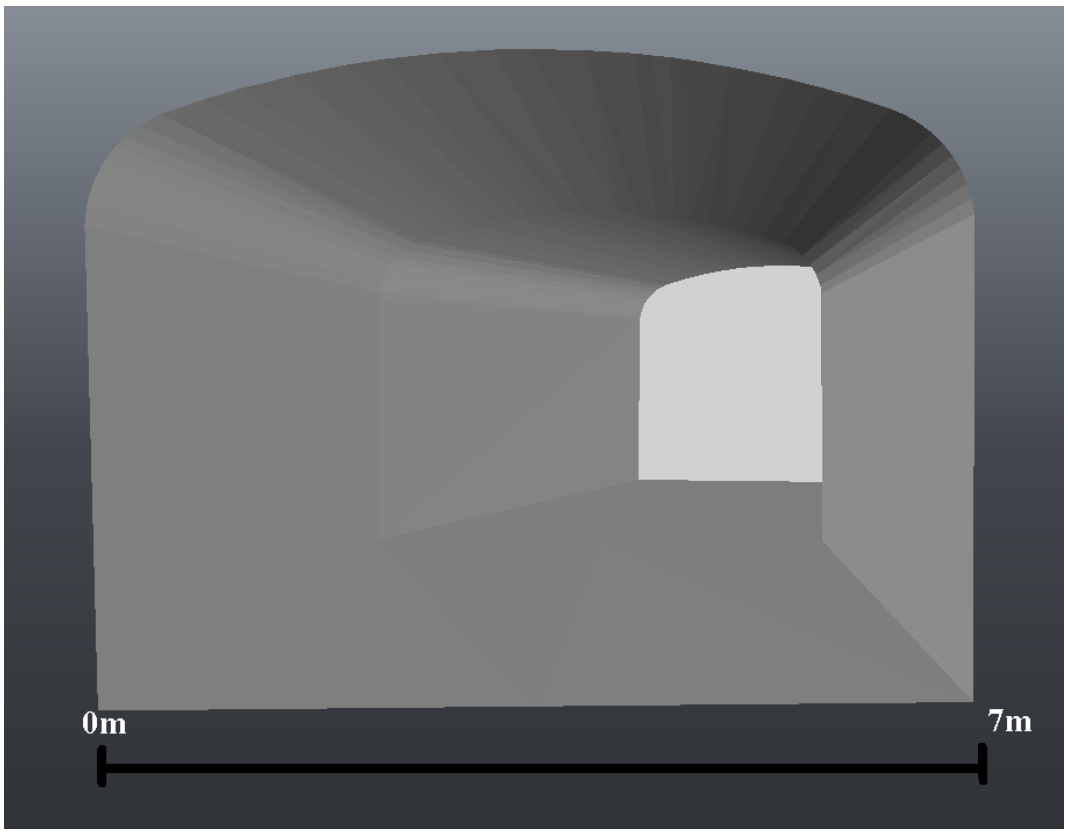

Figure 17. Shows the theoretical model used for volume calculation. The scale is in meters.

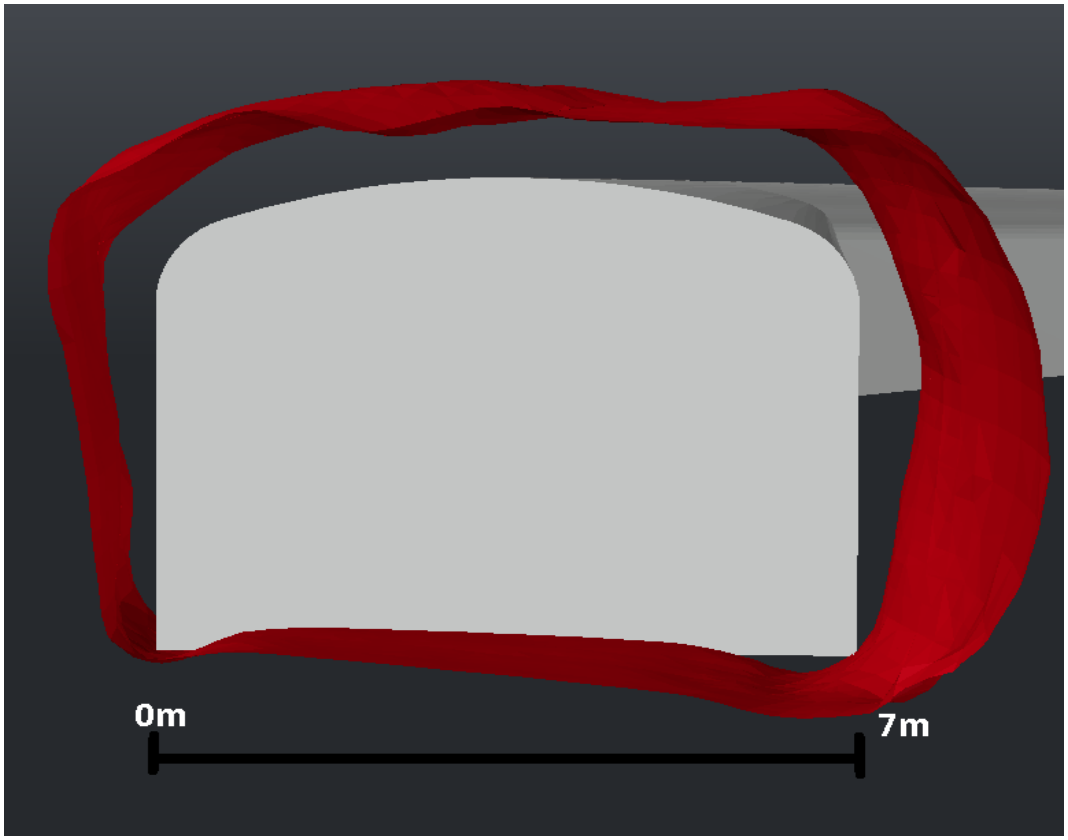

Figure 18. Shows the theoretical model used for volume calculation with a cross section of the mesh produced using Emesent Hovermap placed on top in red color. The scale is in meters.

5 Discussion

5.1 Comparison of point clouds

The appeal of working with SLAM based MLS data over stationary TLS data quickly became apparent with the amount of necessary data processing steps which had to be performed before the Faro TLS data could be presented as a registered point cloud. The software SCENE required each of the twelve scans to be processed individually which would have been a very time-consuming step, had the project contained a larger number of scans. The settings of the automatic registration process then had to be closely inspected, otherwise the entire registration process might have needed to be done over again and finally the quality of the registration had to be acceptable. We have not managed to find any information as to what the accuracy demands for a target- based automatic point cloud registration is. In the end we decided that the values we were given by the SCENE software were accurate enough to be used in generating the Faro point cloud.

Once put into the CloudCompare software the amount of noise outside of the tunnel present in the Faro point cloud compared to the Hovermap point cloud can be seen in appendix C, this also meant that more time had to be spent on trimming and segmenting the Faro point cloud. After segmenting off the roof of the tunnels it is very easy to identify the exact positions where each of the Faro scans were captured which can be seen in appendix E. It is also easy to see what Singh et al. (2023) describes as blind spots in the segments of the tunnel that are the furthest away from the TLS positions.

Both point clouds had their own challenges during the georeferencing stage, the blind spots in the Faro point cloud made it difficult to identify reference point spheres and in some details only became visible from certain viewing angles due to the distance to the nearest visible scanner position. The lower point density in the Emesent Hovermap point cloud made it much more difficult for the software to detect and identify the center of the reference spheres. Several times the software would believe that points behind or around the reference sphere were part of the sphere and display either incorrect sphere radii or displace the center of the sphere. To minimize this error the viewing angle had to be changed several times in such a way that the points of the spheres were visually standing out from the surrounding points.
The stage in which meshes were created to calculate volumes proved easier than what we had expected. We feared that the blind spots in the Faro point cloud would prove troublesome in this stage of the project, but the automated process of the software was able to create meshes out of both point clouds without any issues.

5.2 Interpretation of results

Going into this bachelor's thesis it was believed that the Emesent Hovermap MLS would produce data that would be on par with that of the Faro TLS. However, it became clear early on that the lower point density of the Emesent Hovermap point cloud resulted in great difficulties when it became time to georeference the point cloud. The spheres became difficult to spot within the point cloud and the automated sphere detection feature of the software struggled to accurately find the center of each sphere. This resulted in reference point coordinates being placed next to the spheres which center coordinate they were supposed to represent, rather than in the center of them.

The high RMS values from the Hovermap georeferencing is likely a result of the difficulties of visually and automatically identifying the target reference point spheres, as well as drifting in the point cloud. This becomes very clear based on the fact that the Hovermap yielded a planar accuracy error of 21 millimiters which is roughly 4 times larger than the 4.8 millimeters planar accuracy error the Faro georeference resulted in.

Figure 12 and figure 16 show how the Hovermap point cloud is slightly shifted towards the east which would correspond with the 21 millimeter mean distance between points in the two different point clouds. The reason as to why the Hovermap point cloud is shifted towards the east is most likely due to point cloud drift as explained by Keitaanniem et al. (2023). The Hovermap point cloud was not subject to a loop closure, which increases the chance for drifting in the point cloud. It is possible to reduce the amount of drifting during the post process steps, provided you have the correct software knowledge. Unfortunately, we were unable to find any guides explaining how this was done with software we had access to.

Clear visual differences can be seen when comparing the point cloud from the Faro TLS and the Hovermap MLS. Figure 9 a and b contain the same area of the point clouds produced with Faro TLS and Hovermap MLS. It is clear there are details missing in the Hovermap MLS that are present in the Faro TLS, the sign is legible in the Faro TLS while it is illegible in the Hovermap MLS, this is something to take into consideration if text in the point clouds is to be used as references. The spheres that were used for the georeferencing are easier to identify in the Faro TLS than in the Hovermap TLS meaning georeferencing accurately is an easier task. However, another comparison in figures 10 and 11 show the importance of planning when using TLS to avoid setting up the laser scanner where its view will be obstructed, causing blind spots like the ones mentioned in Singh et al. (2021). In figure 10 depicting the point cloud produced by the Faro TLS the sphere representing the

reference point is quite hard to distinguish and the writing on the wall that is meant to tell the user which reference point they are looking at is illegible. As can be seen in figure 13, one of the reference points in the Faro point cloud has been somewhat obstructed by a total station, it is still useable but less reliable than some of the others. This issue is easier to avoid with a SLAM based MLS as it continuously scans and registers and does not miss spots due to obstruction from one angle. The issue with blind spots may be caused in the registration process or it may be down to the positioning of the laser scanners, as in this area the distance between the scan setups is quite large and the surface on the wall is far from smooth. The Hovermap does not have these issues as it continuously scans hundreds of thousands of points each second while moving.

When doing a side-by-side comparison it becomes evident that the Hovermap MLS cloud is the noisier of the two. The cloud is filled with noise, i.e points that don't exist. This is also evident in figure 8 where the distance between the points in the two point clouds is presented. There are points that have a distance deviation of almost 2 decimeters which is believed to be caused by noise and or rocks in the area. As the area is trafficked by vechicles and personnel and the measurements took place on different days, it is not impossible that objects have shifted between the two measuring days causing these outliers. It is however apparent in figure 8 that only a handful of outliers are left.

As is to be expected, the Faro TLS after visual inspection produced the objectively highest quality point cloud. The Faro TLS point cloud contains roughly 234 million points while the Hovermap MLS point cloud contains roughly 153 million points. It also, however, required over 10 times as long as the Hovermap MLS to gather the required points to produce this result.

Figure 12 shows the overlap between the two-point clouds, and it is visible that the darker Hovermap point cloud is predominant towards the east side of the model. This is most likely a result of the Hovermap point cloud having a larger RMS value which may cause the entire point cloud to shift slightly in a direction. As can be seen in the results section, the largest errors occur in the plane for the Hovermap. The RMS value of around 21 mm is shown to largely be caused by a positive shift in X and Y axis which coincides with figure 12. Even if the shift in coordinates is small enough to not distort the model it is large enough to make a visual distinction when the two-point clouds are placed on top of each other.
When looking at the coordinate deviations presented in figure 4 and 5 it is difficult to detect any clear pattern, it is however clear that there are outliers. In the Faro point cloud the georeferenced Y coordinate deviates from the reference by roughly

16.8 mm which is substantially larger than the other errors present in the Faro point cloud. When inspecting this reference point, it appears to have good scan coverage, although as it is located in a location incline it has been scanned from two different elevations which may have caused an error in the registration process. The laser scanner may have been set up in such a way that the angle at which it scanned is too high to get a good result. It is also possible that the deviation is caused by user error in the post processing stage when identifying the sphere representing the reference point.

In the Hovermap point cloud the X coordinate for point 40269 deviates roughly 44 mm from the reference point. The X coordinate appears to almost always have the largest deviation in the Hovermap point cloud. This supports the idea that the Hovermap cloud has been influenced by SLAM drift which was also shown in figure 16. The deviation was calculated by subtracting the georeferenced coordinate from the reference point, as such a negative value indicates that the georeferenced coordinate is larger. User error in the post processing stage when identifying the spheres may have enhanced or caused the errors present as there were difficulties locating the spheres due to the Hovermaps lower point cloud density.

There are large differences in results of the volume calculation carried out on the point clouds and the volume calculation on the theoretical model as can be seen in table 4. The theoretical model is not normally used as a base for volume calculation, rather it is used to get rough dimensions of the proposed tunnel. It does not take into consideration the surface deformation caused during excavation inside the tunnel as can be seen in figure 17. The theoretical model was brought up as a reference as there was no information regarding the actual volume in the data set provided. As such neither of the point clouds produced a volume close to the theoretical volume. When the two-point clouds are compared the Hovermap point cloud is closer to the theoretical volume but only by about 100 m^3 which is about a 1 % difference. Although the differences seem small, without a known volume it is impossible to determine which is the most accurate and whether the deviation is significant or not depends entirely on its intended use. It is believed the deviation in calculated volume is caused by the mesh creating plugin incorrectly filling the blind spots in the Faro point cloud. With more specialized softwares, like Deswik, it may be possible to acquire more accurate and detailed volume calculations. Our contact person at BLÅ Projekt, Process & GIS AB told us that they usually don't perform volume calculations and as such were unable to provide us with instructions as to how to proceed. It is possible that if we had more experience or access to specialized software like Deswik, the calculated volume of the theoretical model would likely have been closer to the calculated volumes of the two-point clouds.

6 Conclusions

After performing the case study for the bachelor's thesis, we have drawn the following conclusions regarding our research questions:

The laser scanners both have advantages and disadvantages and require different amounts of time for preparation. Faro Focus 3D X 330 TLS produced the point cloud with the highest quality. The difference in point density is evident when the two-point clouds are placed next to one another. Details that are visible in the Faro Focus 3D X 330 TLS point cloud are sometimes lost due to the lack of points in the Emesent Hovermap point cloud. Whether these details are important depends on the purpose of the production of the point cloud. It is worth mentioning that the importance of properly planning the placement of the laser scanners when using TLS cannot be understated. As shown in this case study, incorrect placement leading to obstruction of laser pulses can lead to blind spots which could drastically reduce the quality of the georeferencing and lead to other issues. It is our experience that working with a point cloud with higher point density alleviates the post processing process as details needed for georeferencing are more easily identifiable for both the user and the software.

When reviewing the results, it is evident that the point cloud produced using the Emesent Hovermap MLS is affected by SLAM drift. The RMS values are far greater than the ones in the point cloud produced using Faro TLS and their orientation is the same for all points. It is the opinion of the authors that by utilizing loop closure and using a similar process to the one described in Keitaanniem et al. (2023) that the RMS values can be brought to a more acceptable level and may even be in line with TLS.

While we were unable to acquire a reliable volume calculation from the theoretical model, we could still draw the conclusion that the small difference in the calculated volumes between the two-point clouds is negligible and most likely is a result of the blind spots present in the Faro point cloud. As such we believe that there is no distinction in the quality or reliability between the two targeted laser scanners regarding creating meshes with which volume calculations are made.

As to the best of the authors knowledge, no definitive quality requirement exists for 3D mapping mining tunnels. Rather it depends on the intended use of the point cloud. This study shows that should the intended use be volume calculation, a deviation of around 1 % between the two methods is to be expected and should the intent with creating a 3D map of a mining tunnel be to georeference it to an outer reference system, so that it is connected to other parts of the mine, lower coordinate deviations can be expected from a Faro TLS than a Hovermap MLS. It will however require more time to produce. As such, for each intended use pros

and cons must be weighed against one another before the most suited method can be determined.

7 Future studies

The development and implementation of SLAM based laser scanning has been a complete game changer in the mining industry and the capabilities this technology brings has only begun to be explored. By further studying the difference in quality between SLAM techniques and more standard techniques like TLS, a better understanding on how to further improve and use SLAM based MLS can be acquired. For future studies it would be interesting to compare the Emesent Hovermap with a more modern TLS like the Faro Focus Premium Laser Scanner that was released in 2022.

Should a similar case study be conducted, we would recommend the following changes:

- Position and measure checkpoints in the area to be mapped to allow for better quality controls after performing the georeferencing.
- Shorter distances between the stationary laser scanner positions to eliminate the appearing of blind spots.
- Performing a loop closure on the MLS point cloud to minimize the SLAM drift.
- Acquiring licenses or trial versions of specialized software like Deswik to allow for more reliable results.

References

Ebadi, K., Bernreiter, L., Biggie, H., Catt, G., Chang, Y., Chatterjee, A., Denniston, C. E., Deschênes, S., Harlow, K., Khattax, S., Nogueira, L., Palieri, M., Petrácek, P., Petrlík, M., Reinke, A., Krátký, V., Zhao, S., Agha-mhammadi, A., Alexis, K., Heckman, C., Khosoussi, K., Kottege, N., Morell, B., Hutter, M., Pauling, F., Pomerleau, F., Saska, M., Scherer, S., Siegwart, R., Williams, J. L., & Carlone, L. (2022) Present and Future of SLAM in Extreme Underground Environments. *IEEE Transactions on Robotics*. https://arxiv.org/abs/2208.01787

Ellman, A., Kütimets, K., Varbla, S., Väli, E., Kanter, S. (2021) Advancements in underground mine surveys by using SLAM- enabled handheld laser scanners. *Survey Review*, *volume*(54), 363-374. https://doi.org/10.1080/00396265.2021.1944545

Emesent. (2022). HOVERMAP ST RANGE [Brochure]. https://emesent.com/wp-content/uploads/2023/02/Hovermap-ST-Range-brochure.pdf

Evers, C., & Naylor, P. A. (2018). Acoustic SLAM. *IEEE/ACM Transactions on Audio, Speech, and Language Processing, volume*(26), 1484-1498. http://dx.doi.org/10.1109/TASLP.2018.2828321

Fahle, L., Holley, E. A., Walton, G., Petruska, A. J., & Brune, J. F. (2022) Analysis of SLAM-Based Lidar Data Quality Metrics for Geotechnical Underground Monitoring. *Mining, Metallurgy &Exploration, volume*(39), 1939-1960. https://doi.org/10.1007/s42461-022-00664-3

FARO. (2015). FARO Laser Scanner Focus3D X 330 [Brochure]. https://downloads.faro.com/index.php/s/wG7fpekQexTiZtW

Gollob, C., Ritter, T., & Nothdurft, A. (2020). Forest Inventory with Long Range and High Speed Personal Laser Scanning (PLS) and Simultaneous Localization and Mapping (SLAM) Technology. *Remote sensing, volume(12).* https://doi.org/10.3390/rs12091509

Kazerouni, I, A., Fitzgerald, L., Dooly, G., & Toal, D. A survey of state-of-the-art on visual SLAM. *Expert Systems with Applications, volume*(205).
https://doi.org/10.1016/j.eswa.2022.117734

Kazhdan, M., Bolitho, M., & Hoppe, H. (2006). Poisson Surface Reconstruction. *Eurographics Symposium on Geometry Processing.*
https://www.cs.jhu.edu/~misha/MyPapers/SGP06.pdf

Keitaanniemi, A,. Rönnholm, P., Kukko, A., & Vaaja, M, T. (2023) Drift analysis and sectional post-processing of indoor simultaneous localization and mapping (SLAM)-based laser scanning data. *Automation in Construction, volume*(147).
https://doi.org/10.1016/j.autcon.2022.104700

Kekec, B., BİLİM, N., Karakaya, E., & Ghiloufi, Dhikra. (2021). APPLICATIONS OF TERRESTRIAL LASER SCANNING (TLS) IN MINING: A REVIEW. *Turkey Lidar Journal, volume*(3), 31-38.
http://dx.doi.org/10.51946/melid.927270

Lantmäteriet. (2015). Handbok i mät- och kartfrågor, Terrester Laserskanning 2015. https://www.lantmateriet.se/globalassets/om-lantmateriet/var-samverkan-med-andra/hmk/handbocker/hmk-terrester_laserskanning_2015.pdf

Lantmäteriet. (2017). Handbok i mät- och kartfrågor, Geodatakvalitet 2017. https://www.lantmateriet.se/globalassets/om-lantmateriet/var-samverkan-med-andra/hmk/handbocker/geodatakvalitet-2017.pdf

Lantmäteriet. (2021). Handbok i mät- och kartfrågor, Terrester Laserskanning 2021. https://www.lantmateriet.se/globalassets/om-lantmateriet/var-samverkan-med-andra/hmk/handbocker/hmk-terlas_2021.pdf

Liu, W., Sun, W., Wang, S., & Liu, Y. (2021) Coarse registration of point clouds with low overlap rate on feature regions. *Signal Processing: Image Communication, volume*(98).
https://doi.org/10.1016/j.image.2021.116428

Nam, D. V., & Gon- Woo, K. (2021). Solid- State LiDAR based- SLAM: A Concise Review and Application. *2021 IEEE International Conference on Big Data and Smart Computing (BigComp).*
http://dx.doi.org/10.1109/BigComp51126.2021.00064

Rakotosaona, M. J., Babera, V. L., Guerrero, P., Mitra, N. J., & Ovsjanikov, M. (2019). PointCleanNet: Learning to Denoise and Remove Outliers from Dense Point Clouds. *COMPUTER GRAPHICS Forum.*
https://doi.org/10.48550/arXiv.1901.01060

Ramezani, M., Kjosoussi, K., Catt, G., Moghadam, P., Williams, J., Borges, P., Pauling, F., & Kottege, N. (2022). Wildcat: Online Continuous- Time 3D Lidar- Inertial SLAM. *IEEE TRANSACTIONS ON ROBOTICS.*
https://doi.org/10.48550/arXiv.2205.12595

Reshetyuk, Y. (2006). Investigation and calibration of pulsed time-of-flight terrestrial laser scanners. *Royal Institute of Technology (KTH).*
http://kth.diva-portal.org/smash/get/diva2:10841/FULLTEXT01.pdf

Singh, S. K., Banejee, B. P., & Raval. S. (2023) A review of laser scanning for geological and geotechnical applications in underground mining. *International Journal of Mining Science and Technology, volume*(33), 133-154.
https://doi.org/10.1016/j.ijmst.2022.09.022

Tourani, A., Bavle, H., Sanchez- Lopez, J. L., & Voos, H. (2022). Visual SLAM: What Are the Current Trends and What to Expect?. *Sensors, volume*(22).
https://doi.org/10.3390/s22239297

Van der Merwe, J. W., & Andersen, D. C., (2012) APPLICATIONS AND BENEFITS OF 3D LASER SCANNING FOR THE MINING INDUSTRY. *The Southern African Institute of Mining and Metallurgy.*
https://www.saimm.co.za/Conferences/Pt2012/501-518_vdMerwe.pdf

Whyte, H. D., & Bailey, T. (2006). Simultaneous Localization and Mapping: Part 1. *IEEE Robotics &Automation Magazine,* 99-108.
https://everobotics.org/pdf/SLAMTutorial.pdf

Zhi, Y., Zhang, Y., Chen, H., Yang, K., & Xia, H. (2016). A Method of 3D Point Cloud Volume Calculation Based on Slice Method. *Advances in Computer Science Research*.

http://dx.doi.org/10.2991/icca-16.2016.35

Appendix A

Figure A1 The Faro Laser Scanner Focus 3D X 330 TLS device.

Figure A2. The Emesent Hovermap MLS device.

Appendix B

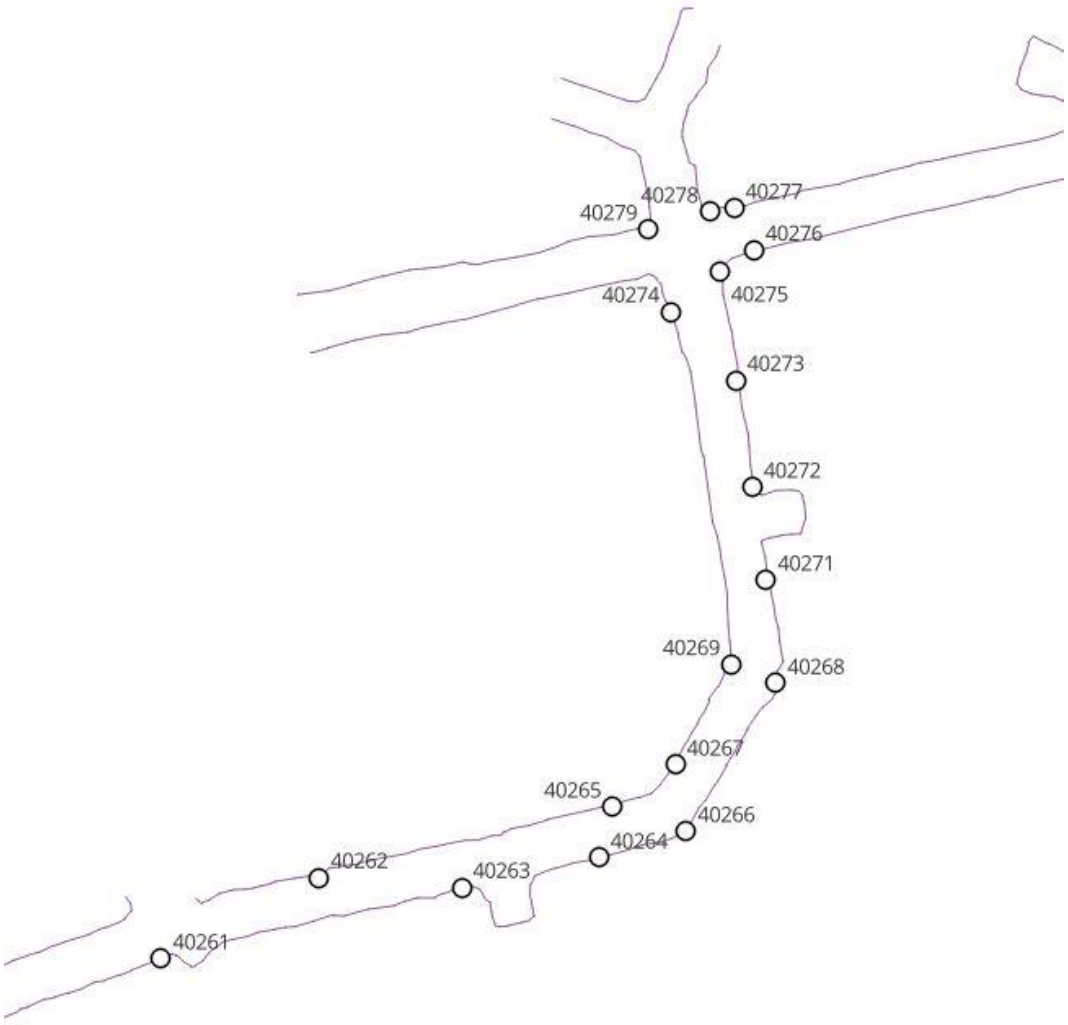

Figure B1. Map of reference points provided by BLÅ Projekt, Process & GIS AB. The scale for this figure is unknown.

Appendix C

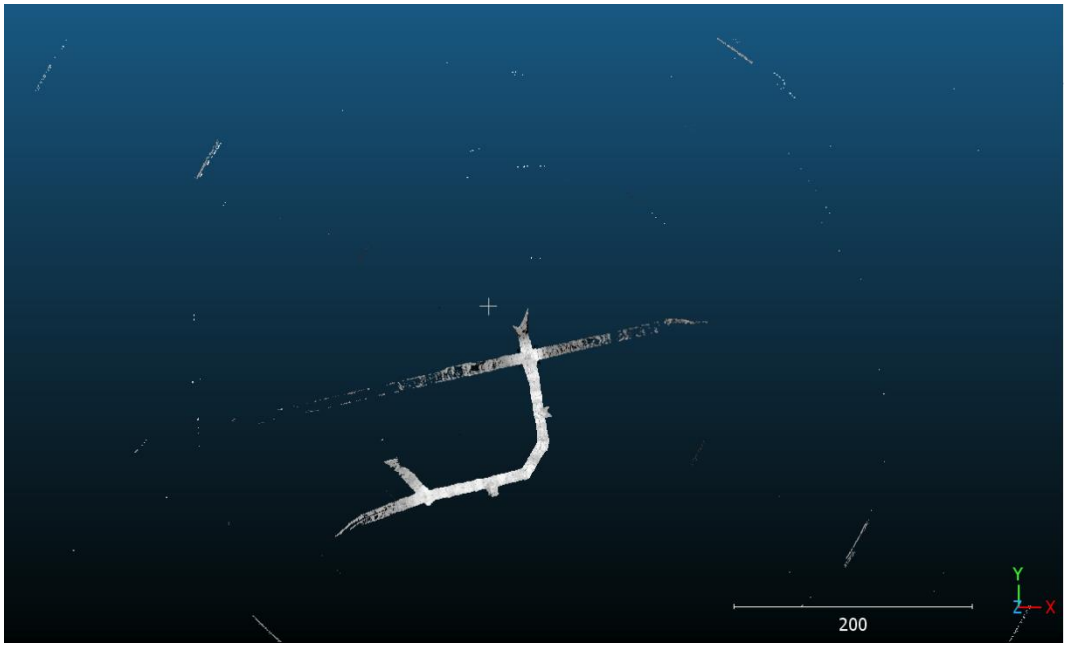

Figure C1. Unsegmented Faro point cloud displayed in CloudCompare. The scale is in meters.

Figure C2. Unsegmented Hovermap point cloud displayed in CloudCompare. The scale is in meters.

Appendix D

Table D1. Shows the coordinates of the georeferenced spheres in the Faro Laser Scanner 3Dx 330 X point cloud in the mine's local coordinate system. The unit is meters.

Point ID	Georeferenced Faro Laser Scanner 3Dx 330 X, Y, Z coordinates (m)			Deviations from reference X, Y, Z coordinates (mm)		
40261	791.3846	6135.5566	-1363.7197	0,36	3,36	-0,27
40262	818.3833	6149.4423	-1367.4222	-1,30	-2,38	2,24
40263	842.8513	6147.7626	-1370.2546	-3,32	7,31	-5,36
40264	866.2060	6152.7968	-1373.8967	0,95	-16,88	-3,27
40265	868.5256	6161.4995	-1374.4600	-0,64	0,49	0,08
40266	881.1416	6157.3271	-1375.0601	-1,60	-7,15	0,18
40267	879.2548	6168.7016	-1375.9487	-0,82	-1,66	-1,27
40268	896.4544	6182.7485	-1377.2357	-0,47	1,47	-4,28
40269	888.8269	6185.8603	-1377.1437	-2,90	-0,35	-6,20
40271	894.8220	6200.2875	-1377.8776	-2,02	2,40	-2,31
40272	892.4154	6216.1669	-1378.7161	1,60	3,01	-3,81
40273	889.5672	6234.4560	-1379.1257	0,80	3,95	-4,27
40274	878.4497	6246.1933	-1379.4810	4,29	-3,36	1,08
40275	886.8207	6253.0639	-1379.4537	5,26	-3,97	3,74
40277	889.2778	6263.8662	-1378.9836	3,17	-6,21	3,64
40278	885.0899	6263.2392	-1379.3641	4,10	-4,26	-1,86
40279	874.6821	6260.2368	-1378.5750	4,81	-4,82	-1,93

Table D2. Shows the coordinates of the georeferenced spheres in the Faro Laser Scanner 3Dx 330 X point cloud in the mine's local coordinate system. The unit is meters.

Point ID	Georeferenced Emesent Hovermap X, Y, Z coordinates (m)			Deviations from reference X, Y, Z coordinates (mm)		
40261	791.3750	6135.5757	-1363.7336	9,94	-15,68	13,64
40262	818.3899	6149.4209	-1367.4138	-7,95	19,10	-6,18
40263	842.8663	6147.7661	-1370.2622	-18,39	3,89	2,21
40264	866.2222	6152.7983	-1373.9021	-15,23	-18,34	2,10
40265	868.5487	6161.4907	-1374.4721	-23,77	9,28	12,17
40266	881.1447	6157.3184	-1375.0678	-4,78	1,64	7,87
40267	879.2826	6168.6758	-1375.9625	-28,65	24,22	12,52
40268	896.4735	6182.7417	-1377.2464	-19,57	8,30	6,46
40269	888.8680	6185.8472	-1377.1550	-44,04	12,83	5,03
40271	894.8244	6200.2925	-1377.8820	-4,40	-2,48	2,08
40272	892.4193	6216.1650	-1378.7211	-2,31	4,96	1,19
40273	889.5536	6234.4575	-1379.1389	14,35	2,48	8,92
40274	878.4487	6246.2095	-1379.4803	5,21	-19,47	0,35
40275	886.8092	6253.0776	-1379.4638	16,74	-17,64	13,87
40277	889.2687	6263.8701	-1378.9888	12,20	-10,12	8,89
40278	885.0770	6263.2334	-1379.3621	16,97	1,60	-3,82
40279	874.6890	6260.2275	-1378.5704	-2,09	4,46	-6,57

Appendix E

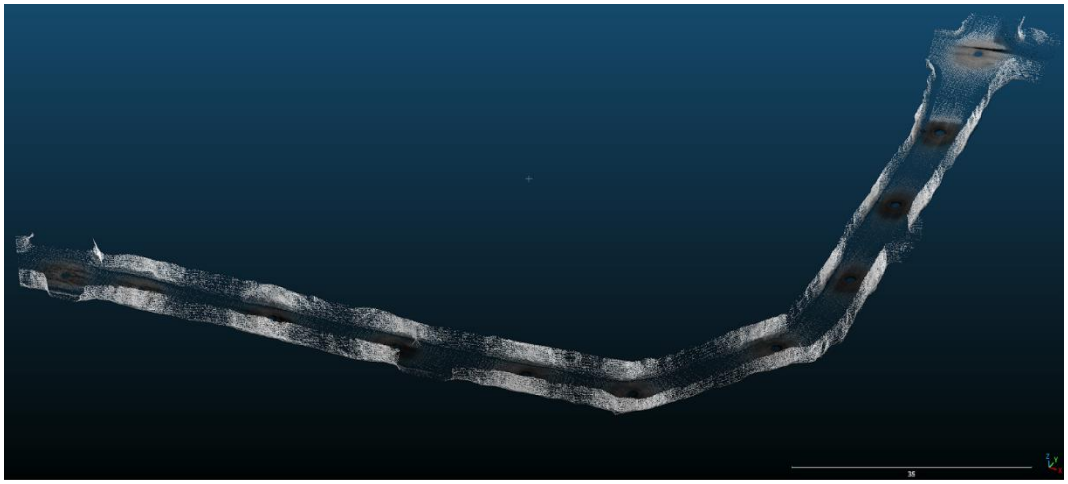

Figure E1. Segmented Faro point cloud displayed in CloudCompare. The unit is meters.

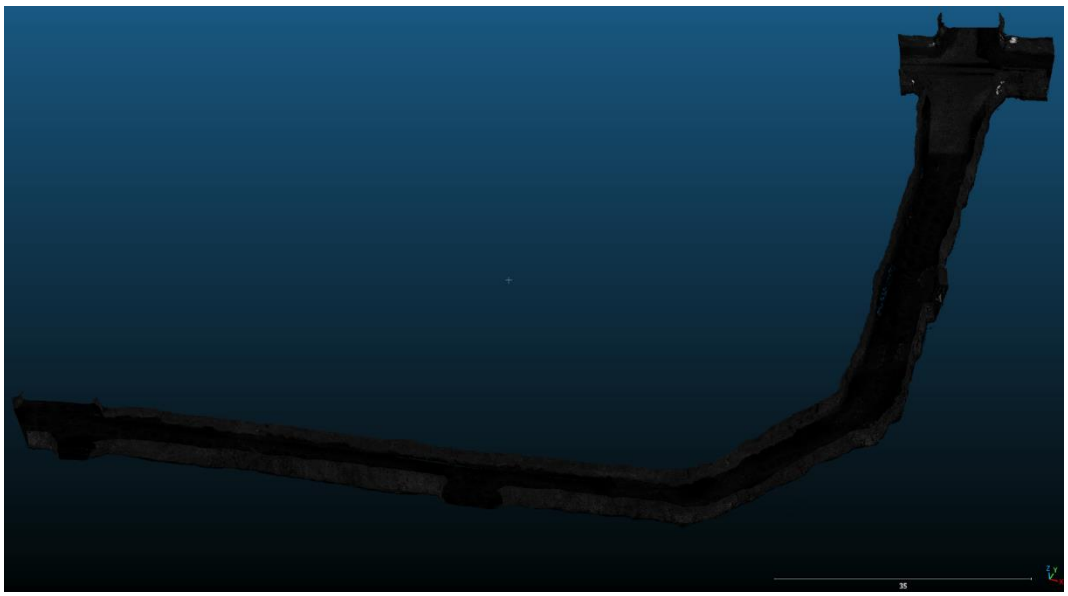

Figure E2. Segmented Hovermap point cloud displayed in CloudCompare. The unit is meters.

Appendix F

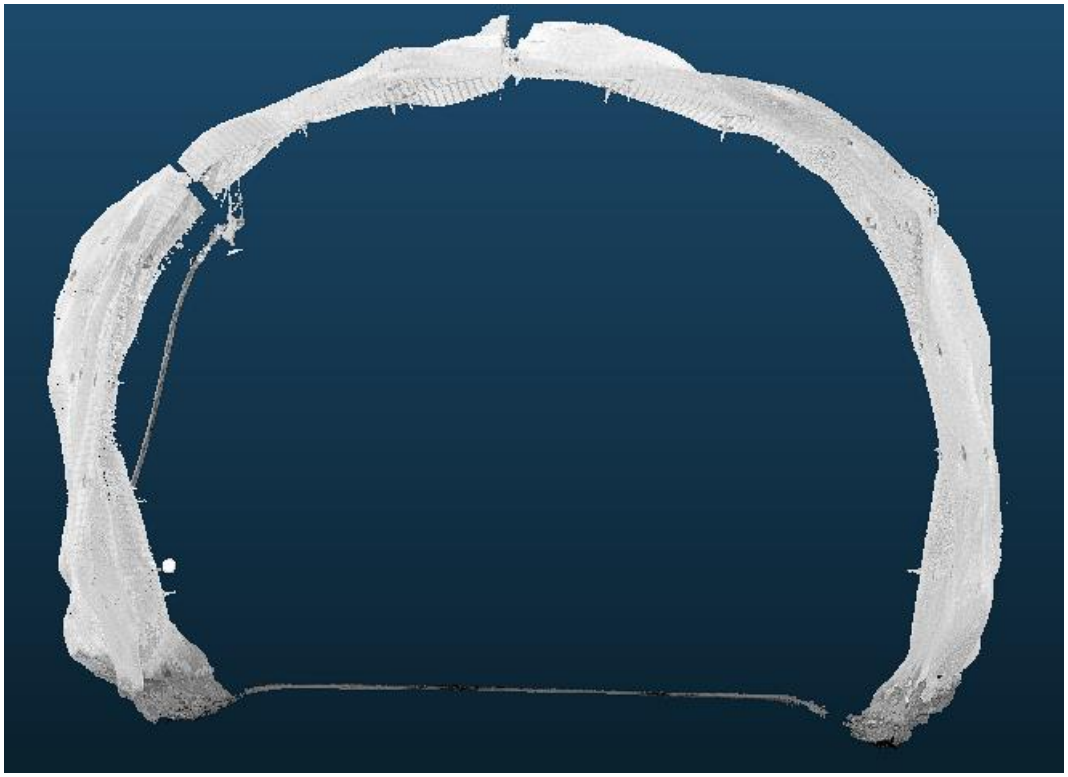

Figure F1. Cross section taken at reference point 40262 in the Faro point cloud displayed in CloudCompare.

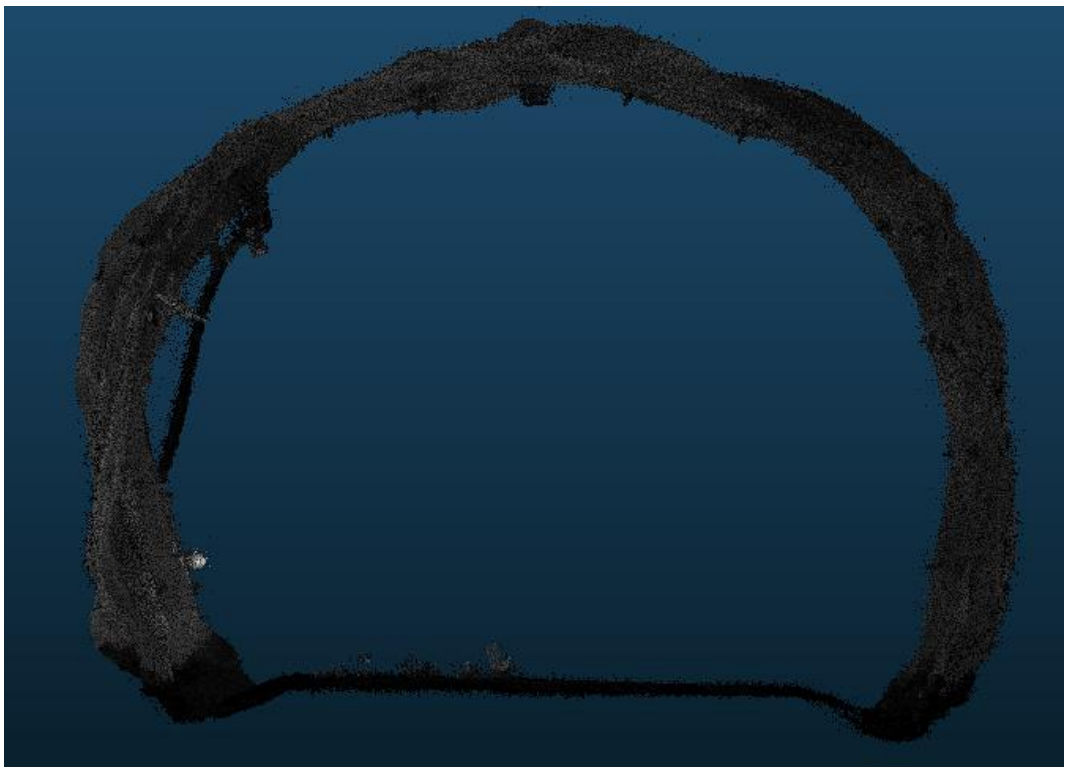

Figure F2. Cross section taken at reference point 40262 in the Hovermap point cloud displayed in CloudCompare.